HYBRID NON-LINEAR MODEL PREDICTIVE CONTROL OF A RUN-OF-MINE ORE GRINDING MILL CIRCUIT

by

Stefan Botha

Submitted in partial fulfilment of the requirements for the degree
Master of Engineering (Electronic Engineering)

in the

Department of Electrical, Electronic and Computer Engineering
Faculty of Engineering, Built Environment and Information Technology

UNIVERSITY OF PRETORIA

January 2018

SUMMARY

HYBRID NON-LINEAR MODEL PREDICTIVE CONTROL OF A RUN-OF-MINE ORE GRINDING MILL CIRCUIT

by

Stefan Botha

Supervisor(s):	Prof. I.K. Craig and Dr J.D. le Roux
Department:	Electrical, Electronic and Computer Engineering
University:	University of Pretoria
Degree:	Master of Engineering (Electronic Engineering)
Keywords:	Advanced process control, Comminution, Genetic algorithm, Grinding mill, Hydrocyclone cluster, Hybrid modelling, Hybrid non-linear model predictive control, Milling

A run-of-mine (ROM) ore milling circuit is primarily used to grind incoming ore containing precious metals to a powder fine enough to liberate the valuable minerals contained therein. The ground ore has a product particle size specification that is set by the downstream separation unit. A ROM ore milling circuit typically consists of a mill, sump and classifier (most commonly a hydrocyclone). These circuits are difficult to control because of unmeasurable process outputs, non-linearities, time delays, large unmeasured disturbances and complex models with modelling uncertainties. The ROM ore milling circuit should be controlled to meet the final product quality specification, but throughput should also be maximised. This further complicates ROM ore grinding mill circuit control, since an inverse non-linear relationship exists between the quality and throughput.

ROM ore grinding mill circuit control is constantly evolving to find the best control method with peripheral tools to control the plant. Although many studies have been conducted, more are continually undertaken, since the controller designs are usually based on various assumptions and the required measurements in the grinding mill circuits are often unavailable.

To improve controller performance, many studies investigated the inclusion of additional manipulated variables (MVs) in the controller formulation to help control process disturbances, or to provide some form of functional control. Model predictive control (MPC) is considered one of the best advanced process control (APC) techniques and linear MPC controllers have been implemented on grinding mill circuits, while various other advanced controllers have been investigated and tested in simulation. Because of the complexity of grinding mill circuits non-linear MPC (NMPC) controllers have achieved better results in simulations where a wider operating region is required.

In the search for additional MVs some researchers have considered including the discrete dynamics as part of the controller formulation instead of segregating them from the APC or base-layer controllers. The discrete dynamics are typically controlled using a layered approach. Discrete dynamics are on/off elements and in the case of a closed-loop grinding mill circuit the discrete elements can be on/off activation variables for feed conveyor belts to select which stockpile is used, selecting whether a secondary grinding stage should be active or not, and switching hydrocyclones in a hydrocyclone cluster.

Discrete dynamics are added directly to the APC controllers by using hybrid model predictive control (HMPC). HMPC controllers have been designed for grinding mill circuits, but none of them has considered the switching of hydrocyclones as an additional MV and they only include linear dynamics for the continuous elements. This study addresses this gap by implementing a hybrid NMPC (HNMPC) controller that can switch the hydrocyclones in a cluster.

A commonly used continuous-time grinding mill circuit model with one hydrocyclone is adapted to contain a cluster of hydrocyclones, resulting in a hybrid model. The model parameters are refitted to ensure that the initial design steady-state conditions for the model are still valid with the cluster.

The novel contribution of this research is the design of a HNMPC controller using a cluster of hydrocyclones as an additional MV. The HNMPC controller is formulated using the complete non-linear hybrid model and a genetic algorithm (GA) as the solver. An NMPC controller is also designed and implemented as the base case controller in order to evaluate the HNMPC controller's performance. To further illustrate the functional control benefits of including the hydrocyclone cluster as an MV, a linear optimisation objective was added to the HNMPC to increase the grinding circuit throughput, while maintaining the quality specification.

The results show that the HNMPC controller outperforms the NMPC one in terms of setpoint tracking, disturbance rejection, and process optimisation objectives. The GA is shown to be a good solver for HNMPC, resulting in a robust controller that can still control the plant even when state noise is added to the simulation.

ACKNOWLEDGEMENT

I would like to give a great thank you to my study leader Prof. Ian Craig. Without your mentorship and guidance this work would not have been possible. I am grateful for being able to learn from you what makes an excellent researcher and control engineer and I am humbled by the opportunities you gave me.

Thank you to Dr. Derik le Roux for the numerous short notice technical discussions we had and your willingness to always help me grow as a researcher. I am greatly indebted to your contribution towards this work.

Thanks to the National Research Foundation (DAAD-NRF) that mostly funded this research.

Lastly, my sincerest thanks to Johanie and my family. Your love, support, encouragement and belief in me has always been an inspiration for me and for that I am eternally grateful.

LIST OF ABBREVIATIONS

AG	Autogenous grinding
APC	Advance process control
CV	Controlled variable
GA	Genetic algorithm
HNMPC	Hybrid non-linear model predictive control
MLD	Mixed logical dynamical
MPC	Model predictive control
MPSO	Modified particle swarm optimisation
MV	Manipulated variable
NMPC	Non-linear model predictive control
PID	Proportional, integral, derivative
PV	Process variable
RNMPC	Robust non-linear model predictive control
ROC	Rate of change
ROM	Run-of-mine
SAG	Semi-autogenous grinding

TABLE OF CONTENTS

CHAPTER 1 INTRODUCTION

This chapter details the problem context and research gap addressed in this study. A summary is also given of the study objectives, as well as a hypothesis and research questions. The methods to evaluate the hypothesis and answer the research questions are listed. The research contribution highlights the novel approach and relevance of the work and lists the resulting publications. The chapter concludes with an overview of the study by highlighting the focus area of each chapter.

1.1 PROBLEM STATEMENT

1.1.1 Context of the problem

A run-of-mine (ROM) ore milling circuit is used to grind incoming ore bearing precious minerals to within a specification, e.g. 80% of the product particles must be smaller than 75 μm. The fine product produced from the milling circuit allows for the separation of the precious minerals from the gangue in the downstream process [1]. In order to improve the recovery rate of the valuable metals in the downstream processes, the particles discharged from the grinding mill circuit should remain at a quality set by the downstream process [2].

Generally, the better the quality of the product, the lower the throughput of the grinding mill circuit, and vice versa [3]. Because of the inverse relationship between the product quality and throughput, the aim is to maintain quality as close as possible to the specification set by the downstream processes, and then maximise throughput even in the presence of large disturbances [4]. By reducing the fluctuations in quality, the quality setpoint can be set closer to the minimum specification thereby maximising throughput. In addition to these control objectives, a grinding mill circuit controller should also aim to increase energy efficiency and at all times ensure process stability [5, 6].

1.1.2 Research gap

The norm for industrial milling circuit control is single-loop proportional-integral-derivative (PID) controllers despite strong interactions between the loops [7]. Single-loop PID controllers do not easily allow for any trade-off between the control objectives. Therefore, if one of the loops reaches a manipulated variable (MV) constraint, the other loops cannot attempt to offset the resulting setpoint error. A variety of multivariable controllers were developed to achieve the optimal trade-off between the control objectives and improvements in product quality, throughput, and power consumption [2, 6, 8, 9].

Advanced process control (APC) techniques have been implemented in an attempt to control grinding mill circuits effectively. Linear model predictive control (MPC) controllers were developed, which could efficiently control the grinding mill circuit [2, 8]. However the robust non-linear MPC (RNMPC) controller developed in [4] showed that even in the presence of large disturbances and model mismatch it was possible to control a grinding mill circuit efficiently. Non-linear MPC (NMPC) outperformed linear MPC owing to the large non-linearities in the grinding mill circuit that can be handled by the NMPC controller. By being able to use a non-linear model, the controller can operate over a much wider operating region. This is predominantly due to the non-linearities associated with the mill power draw, mill filling and throughput [10]. Linear controllers are therefore restricted to narrow operating regions around the linearised point.

To improve the operating range of grinding mill circuit controllers, not only were APC controllers designed, but additional MVs were identified to be included in the controller. In [11] the range of quality control was increased by independently manipulating the mill's water feed rate instead of fixing the water feed rate as a ratio of the ore feed rate. Similarly, in [12] the range of quality control was increased by manually switching cyclones in a hydrocyclone cluster. Power consumption reduction while maintaining quality was achieved in [13] by alternating between different stockpiles as ore feed and choosing whether a secondary grinding stage would be used or not. In [14] and [15] the mill speed is used as an additional MV to reduce mill power consumption, and to control quality and throughput independently.

Grinding mill circuits often contain a hydrocyclone cluster instead of just one hydrocyclone [16]. As ore feed composition changes, the size of the hydrocyclone cluster can vary (i.e. it could require

more or fewer hydrocyclones) [17]. In order to accommodate sporadic feed ore changes, the cluster of hydrocyclones is designed for the maximum required number of hydrocyclones, and individual hydrocyclones are then switched on or off depending on process requirements[16, 18].

Hybrid model predictive control (HMPC) is capable of controlling a process by predicting continuous- and discrete-time events, and manipulating continuous and discrete components [19, 20]. HMPC has been implemented in grinding mill circuits to illustrate the benefits of including the discrete dynamics as part of the controller formulation as opposed to using a layered approach. In [13] a linear HMPC was implemented to select which stockpile to feed from or if the secondary grinding stage should be active. Similarly, [21] gives a framework for HMPC of grinding mill circuits, where linear steady-state models are considered. These HMPC controllers only considered linear dynamics, but as shown in [4] for a grinding mill circuit, non-linear models are more suitable than linear models. The HMPC controllers did not consider the possibility of switching hydrocyclones in a cluster either.

Therefore the research gap addressed in this study is to improve linear HMPC by implementing a hybrid non-linear MPC (HNMPC) controller to use the switching of hydrocyclones as an additional MV. This will result in a controller that can benefit from controlling over a wider operating region due to the non-linear model and it will be able to directly incorporate hydrocyclone switching as part of the optimal control problem.

1.2 RESEARCH OBJECTIVE AND QUESTIONS

The aim of the study is to expand a grinding model to contain a hydrocyclone cluster that can be used for controller design and simulation, design an HNMPC controller which can sufficiently control the plant using the common continuous time handles and the discrete switching of hydrocyclones, and design a base case NMPC controller to which the HNMPC can be compared. The resulting research questions for this study are:

- Can an available continuous non-linear model be expanded to a hybrid model containing discrete inputs?
- Are there benefits in including discrete dynamics (in the form of switching hydrocyclones) in a predictive controller?

- Is hybrid non-linear model predictive control using a genetic algorithm a feasible solution for controlling grinding mills?
- What are the benefits of hybrid model predictive control over conventional non-linear model predictive control in grinding mill circuits?

1.3 HYPOTHESIS AND APPROACH

The hypothesis in this study is that a HNMPC controller can be used effectively to control a grinding mill circuit while benefiting from using discrete dynamics as an additional controller handle. The switching of hydrocyclones proves to be a good additional handle in situations where the hardness and composition of feed ore to a grinding mill circuit changes and when the quality setpoint is regularly changed.

The approach followed in this study is as follows:

1. Present the body of knowledge concerning grinding mill circuit theory, control philosophy and controllers implemented on them to understand the limitations of the circuit, requirements in modelling, and methods of evaluating the controller performance.
2. Identify a commonly used ROM ore grinding mill circuit model used in control and expand the model to a hybrid model by including a hydrocyclone cluster with on-off valves at the inlet of each hydrocyclone. With the additional switching logic, the parameters of the hydrocyclones are re-fitted to maintain the original operating conditions.
3. Identify a possible solver that can solve non-linear mixed integer problems with hard constraints. The controllers are tuned to be as identical as possible to ensure that any additional benefits result purely from the HNMPC's ability to switch hydrocyclones.
4. Set up a simulation to test whether the HNMPC outperforms the NMPC as a regulatory controller (maintaining setpoints while rejecting disturbances) and whether it can use the additional MV to achieve an optimisation objective (i.e. attempting to use the MVs to maintain setpoints and maximise the circuit throughput).

1.4 RESEARCH GOALS

The research goals can be summarised as follows:

- Successfully expand a ROM ore grinding mill circuit model to a hybrid model containing a hydrocyclone cluster.
- Successfully formulate an HNMPC controller utilising the hybrid model.
- Illustrate the benefits of HNMPC over NMPC for a ROM ore grinding mill circuit.
- Show that the HNMPC can control the ROM ore milling circuit even when state and measurement noise is added to the simulation.

1.5 RESEARCH CONTRIBUTION

A model commonly used in predictive controller and state estimator design was expanded to a hybrid model and the parameters were refitted so that a hydrocyclone cluster could be used in the circuit instead of just one hydrocyclone. The model was validated by showing that identical steady-state conditions are achieved for the initial circuit and the circuit with the hydrocyclone cluster under nominal conditions.

A non-linear HNMPC controller capable of switching hydrocyclones in a cluster was designed and simulated for a grinding mill circuit. Available grinding mill circuit HMPC controllers could only use linear grinding mill circuit models and they did not consider using a hydrocyclone cluster as an MV. Both these gaps were addressed with the new controller. In a simulation with acceptable process noise, it was shown that in cases where the ore feed composition or hardness changes, the switching of hydrocyclones is a valuable additional MV to achieve a more economic operating region over a base case NMPC controller. It was also shown that with the additional MV, optimisation benefits can be achieved with the HNMPC that could not be achieved with the NMPC (i.e. maximising throughput when all other controller variables (CVs) are at their desired setpoints).

The following publications resulted from this work,

- S. Botha, I.K. Craig, and J.D. le Roux, "Switching cyclones to increase product particle size range for ore milling circuits", in IFAC Workshop on Automation in Mining, Minerals and Metal Industry, Oulu, Finland, 25-27 Aug. 2015. IFAC-PapersOnLine, vol 28, issue 17, 2015 pp. 92-97. doi:10.1016/j.ifacol.2015.10.084
- S. Botha, J.D. le Roux, and I.K. Craig, "Hybrid non-linear model predictive control of a run-of-mine ore grinding mill circuit," Submitted to: Minerals Engineering, October 2017.

1.6 OVERVIEW OF STUDY

An overview of the structure of the dissertation is as follows:

1. Chapter 2 gives the body of knowledge relevant to ROM ore grinding mill circuit theory, control philosophy, and modelling. It also discusses hybrid systems, APC of continuous systems and APC of hybrid systems.
2. Chapter 3 presents a continuous time ROM ore grinding mill circuit model. The hydrocyclone model is expanded to a cluster of hydrocyclones containing switching dynamics. All the steps in expanding the model are described, as well as the approach to refitting the model parameters.
3. Chapter 4 presents the formulation of three controllers: a base case NMPC, an HNMPC and an HNMPC with a linear optimisation objective. By designing two HNMPC controllers it can be determined whether including the optimisation objective causes any instabilities and whether throughput can be maximised in certain conditions.
4. Chapter 5 presents the controller simulation results. Performance metrics are presented and used to evaluate each controller's performance. The HNMPC is tested with state/measurement noise in a final simulation.
5. Chapter 6 contains the dissertation conclusion and suggests possible future work.

CHAPTER 2 LITERATURE STUDY

2.1 CHAPTER OVERVIEW

In this chapter, grinding mill circuit control, modelling and state estimation strategies are evaluated. The chapter concludes with a discussion on APC.

2.2 RUN-OF-MINE GRINDING MILL CIRCUIT THEORY

Mineral processing involves all the steps to liberate precious minerals from raw ore into a final product. These steps involve transportation of material to crusher circuits, crushing, grinding, flotation and thickening [22]. Each operating unit is dependent on the efficient operation of the upstream unit. Typically the operating conditions for a processing unit are determined by the requirements of the downstream unit [7].

Grinding mill circuits are commonly the bottleneck in mineral processing and consume most power. Because of high operating costs and energy consumption, the grinding mill is the most expensive step in mineral processing [23]. For this reason, increases in throughput and any cost-saving opportunities for the grinding mill circuit result in considerable economic benefits for the entire mineral processing plant.

A grinding mill circuit is the first step in mineral processing and raw ore is fed directly to the grinding circuit from different stockpiles [16]. These grinding mill circuits are referred to as ROM ore grinding mill circuits. Since the feed ore undergoes no pre-treatment or separation, sporadic changes in feed ore quality are observed.

The grinding of ROM ore to a fine product is achieved through grinding mill circuits. An example of such a circuit is shown in Figure 2.1, which consists of four elements:

- a feeder module,
- a mill, which is the primary grinding element,
- a sump, and
- a classifier, which can be a hydrocyclone (as depicted in Figure 2.1) or a screen separator.

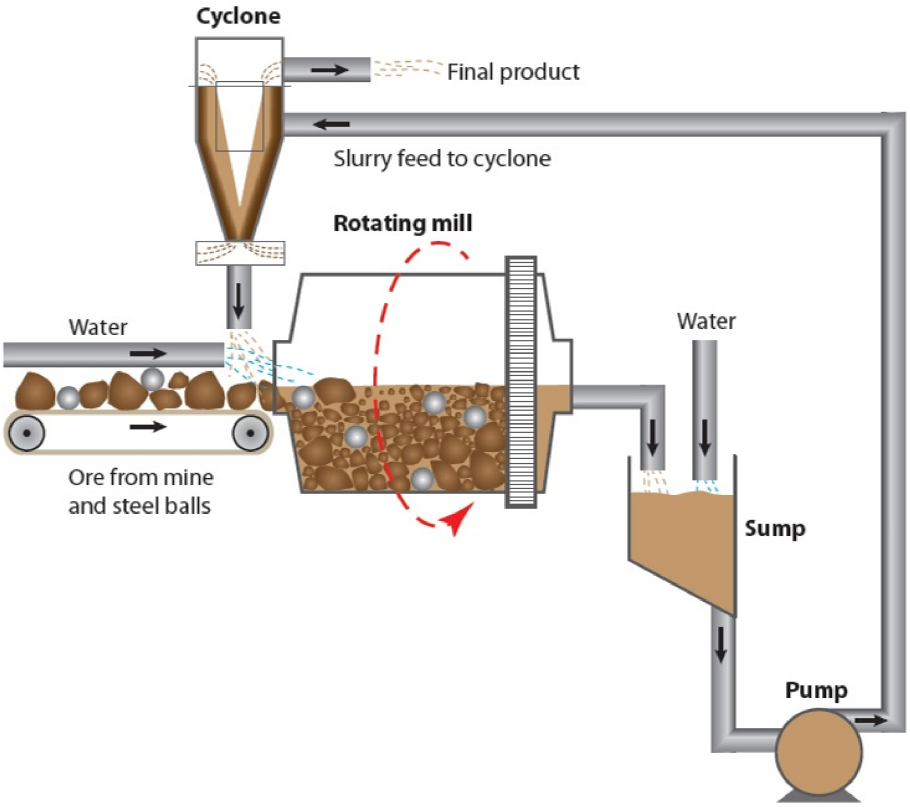

Figure 2.1. A closed-loop single-stage grinding mill circuit.

2.2.1 Milling circuit feed

The feeder module is responsible for feeding precious metal-bearing ore, steel balls (if required depending on the type of mill), additional water and any out-of-specification material from the classifier that requires re-grinding. Typically for a grinding mill circuit designed for gold-bearing ore with a mill that has a length of 9 m and a diameter of 5 m, ore is fed to the mill at a rate of approximately 100 tons per hour [24].

The ROM ore fed into the mill is ground to a fine powder in order to extract the precious minerals in the downstream units. The ROM ore contains a distribution of precious minerals and gangue (worthless material). In gold-bearing ore the volume of gangue is much larger than the volume of valuable minerals. The downstream units separate the minerals from the gangue through physical and/or chemical processes, which require the fine ore to be within specification. In milling "within specification" refers to the fineness of the particles discharged as final product. The grinding circuit does not produce a uniform distribution of particle sizes, in other words the ore is broken down into various different sized smaller particles. The quality of the final product is measured as a percentage of final product particles smaller than the specification size. The quality specification for a gold-bearing ore circuit can be represented as P_{80} = 75 μm, which means 80% of the final product particle size distribution, on a mass basis, should be smaller than 75 μm [25]. The quality specification can vary significantly from one ore type to the other.

2.2.2 Mill

The primary element for grinding the incoming ore is usually a ball, rod, semi-autogenous (SAG) or autogenous (AG) mill [4]. The mill grinds the large ore to smaller particles by rotating the load. Because of the rotation, the grinding medium will lift in the mill to a point where it falls back down and crushes into the load that is not rotating. The impact causes the ore to break down into smaller particles. The point at which the gravitational pull exceeds the rotational force and the ore tumbles downward is referred to as the shoulder. The point where the non-rotating load is closest to the impact is referred to as the toe [16]. This effect is illustrated in Figure 2.2, where the direction of rotation is clockwise. Water is added to assist with the breakage and discharge of sufficiently small particles from the mill. Steel balls (in the case of ball or SAG mills) or steel rods (in the case of a rod mill) are added to the mill to assist with breakage [24].

AG mills use only the mined ore as the grinding medium in the mill. The two most common mills are SAG and ball mills, which use both ore and steel balls as grinding media [7]. Steel balls assist in the breaking of ore in the mill. Ball mills have a much higher ball load than SAG mills [24]. Ball mills are often used where the ROM ore is crushed before being added to the mill; SAG mills require larger ROM ore. Apart from steel balls being added to the mills to assist with the breakage of ore, steel rods can also be used, as is done in rod mills. AG mills are often converted to SAG mills because SAG

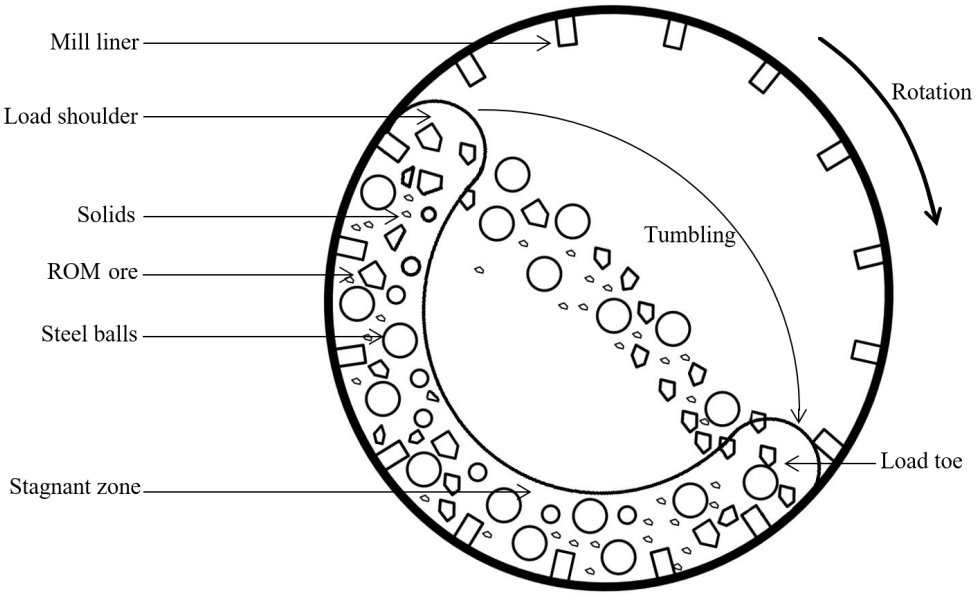

Figure 2.2. Rotation of grinding media in a SAG mill.

mills have a greater throughput [26].

The inner surface of the mill is protected with mill liners, which are important for two reasons; the mill liners protect the outer walls of the mill and they ensure that the shoulder in the mill is high enough to result in efficient grinding. As the liners wear out, the mill characteristics change and could cause the mill to run under sub-optimal conditions requiring liner changing [27]. Liners are considered a consumable and add to the high operating costs of grinding mills. Efficient operation of the mill is therefore important to protect the integrity of the mill liners and reduce maintenance cost due to mill downtime and liner replacement costs [28].

In Figure 2.1 a single-stage closed-loop grinding mill circuit is shown. The design of the milling circuit is dependent on the characteristics of the ore being mined. For harder ore a configuration can require a primary grinding stage, often a SAG mill, which feeds a secondary grinding stage that typically uses a ball mill. In the case where the ore is hard, the residence time required in the mill is greater, and lower throughput of the circuit is expected. In these cases parallel mills are considered. Grinding mill circuits are also designed with mills in parallel to ensure continuous operation when one mill goes down because of electrical motor failure or maintenance as a result of liner wear [16].

The slurry mixture of ground ore and water is discharged from the mill through an end discharge grate

to the sump. The grate ensures that no large rocks are discharged from the mill; however the grate is not designed in such a way that only particles within specification are discharged. Some of the ore may still be out of specification and is fed back to the mill for further grinding [24].

2.2.3 Sump

The sump is a buffer between the mill and the classifier. In the sump the slurry discharged from the mill is further diluted with water. Any disturbances resulting from the mill should be absorbed by the sump to ensure that the feed to the classifier remains constant to ensure efficient operation of the classifier (this is especially important if a hydrocyclone is used) [16].

2.2.4 Classifier

In Figure 2.1 the final classifier is a hydrocyclone. The hydrocyclone separates the in-specification particles from the out-of-specification particles. The in-specification particles are discharged from the hydrocyclone overflow as final product, while the out-of-specification particles are recycled through the hydrocyclone underflow back to the mill for further grinding [1]. The hydrocyclone is designed to ensure the final cut for the grinding mill circuit (for example $P_{80} = 75\ \mu m$) [16].

Hydrocyclones are conically shaped centrifugal separators with an opening at the bottom (at the apex of the cone) called the spigot. The cone is joined to a cylindrical section that contains the inlet. The top of the cylindrical section is closed except for an overflow pipe. The pipe is extended into the body through the vortex finder [24].

The principle of operation for a hydrocyclone is based on the concept of the terminal settling velocity of a solid particle in a centrifugal field. The slurry from the sump is fed tangentially into the hydrocyclone. The material follows a high-velocity circular path, which generates high centrifugal forces in the hydrocyclone. The centrifugal forces create an air-liquid core on the middle axis that extends from the spigot to the vortex finder. Most of the liquid will be suspended in the centre of the hydrocyclone and because of the drag forces required for the larger particles to move to the centre vortex, they remain on the outer walls and gravity pulls the particles to the bottom of the hydrocyclone. The smaller particles can overcome the drag forces and are discharged through the vortex finder as overflow [16].

The capacity of the hydrocyclone is limited by the discharge rate of solids through the spigot opening. If the hydrocyclone feed density is too high and the feed to the hydrocyclone remains constant, the solids content of the underflow increases. This increase results in the viscosity of the underflow to increase, which slows down the tangential velocity and a rope-like stream is discharged from the underflow of the hydrocyclone. This is referred to as roping. During normal operation the cyclone underflow should flare out in an umbrella shape [16].

Grinding mill circuit designs can vary to use a hydrocyclone cluster instead of just one hydrocyclone. A hydrocyclone cluster allows for smaller cyclones, while maintaining high volumetric flow rates, to achieve a finer cut [22]. In addition hydrocyclone clusters are beneficial for circuits where the circulating load in the circuit can often change [17]. These changes can result from feed disturbances such as changes in the ore hardness, or as a result of process conditions (i.e. one mill taken off-line for maintenance).

By including a hydrocyclone cluster the circuit is made more robust to changing process conditions and the switching of hydrocyclones in the cluster makes it possible always to maintain the correct feed pressure and feed density to the individual hydrocyclones [17].

2.3 OPERATING PHILOSOPHY AND CONTROL OF GRINDING MILL CIRCUITS

This section details the operating philosophy of grinding mill circuits, as well as the controllers commonly used.

2.3.1 Operating philosophy

Grinding mill circuits have various control objectives. Grinding mill circuit control should firstly ensure that the process remains stable (given measured and unmeasured plant disturbances) and only then can economic benefits be considered [29]. According to [30] the economic control objectives for a grinding mill can be listed as:

1. improve product quality by

   (a) ensuring the final product size is within specification, and

   (b) reducing fluctuations in final product particle size,

2. maximise throughput,
3. improve mill energy efficiency, and
4. minimise the use of steel balls.

Efficient control of grinding mill circuits is difficult to achieve because of strong loop interactions in the circuit, strong correlations between control objectives, large time delays between the different elements in the grinding mill circuit and the unavailability of process measurements (which is the most important factor to consider).

The biggest trade-off in the circuit is between quality and throughput because of a strong inverse relationship between them. As the product quality increases and a finer final product is produced, the throughput is reduced [7]. However even though a finer product (objective 1a) increases the amount of valuable minerals recovered, fluctuations in particle size reduces the recovery (objective 1b) [6]. Furthermore if the product particle size does not fluctuate, the circuit can operate closer to the minimum quality specification, thereby increasing throughput. Figure 2.3 shows the recovery rate of a flotation unit as a function of the product particle size estimate and clearly shows the sensitivity of the downstream process to the grinding mill circuit. The figure is reconstructed from the recovery performance function given in [31] as,

$$\vartheta = -0.009776 \times PSE^2 + 1.705 \times PSE - 2.955 \tag{2.1}$$

where ϑ is the recovery percentage and PSE is the particle size estimation (percentage of particles smaller than 75 μm).

Obtaining economic benefit by reducing throughput to improve energy efficiency (objective 3) is generally not feasible. Therefore when power conservation control techniques are implemented, a minimum reduction in circuit throughput should be observed [5]. It is often assumed that maximum throughput is achieved when the mill power consumption is maximised [6].

The cyclone feed density, CFD, is not directly controlled but is usually minimised in order to maximise the circulating load in order to increase classifier performance [32].

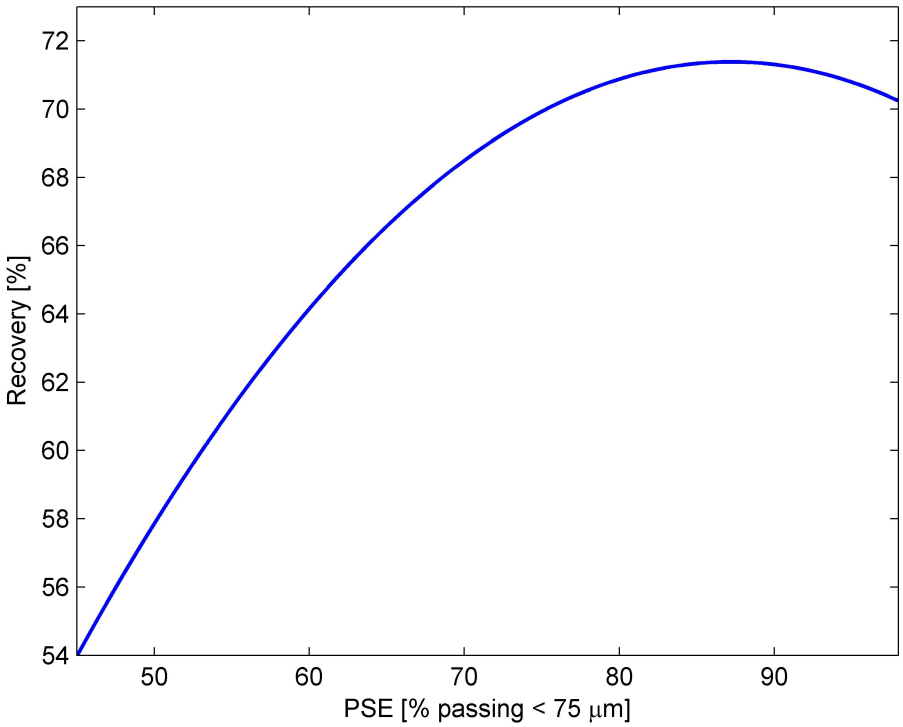

Figure 2.3. Recovery of a flotation unit as a function of PSE.

The typical control philosophy for a grinding mill circuit containing a SAG mill, sump, and hydrocyclone cluster, as depicted in Figure 2.4, can be summarised from [7] as follows:

- The MVs are the feed of ore to the mill (mill feed solids, MFS), the additional water added to the sump (sump feed water, SFW), the hydrocyclone cluster feed flow rate (CFF), the feed rate of water to the mill (mill inlet water, MIW), the feed of balls into the mill (mill feed balls, MFB) and the mill speed.
- Mill load is controlled to setpoint to ensure process stability.
- The level of the slurry in the sump should be controlled over a range to ensure the stability of the hydrocyclone feed and corrective action should be taken when the sump level exceeds a lower or upper limit.
- The product particle size (PSE) should be controlled to a setpoint as required by the downstream separation unit.
- At the given quality specification, throughput should be maximised, which is commonly achieved through peak-seeking control for maximum power usage.

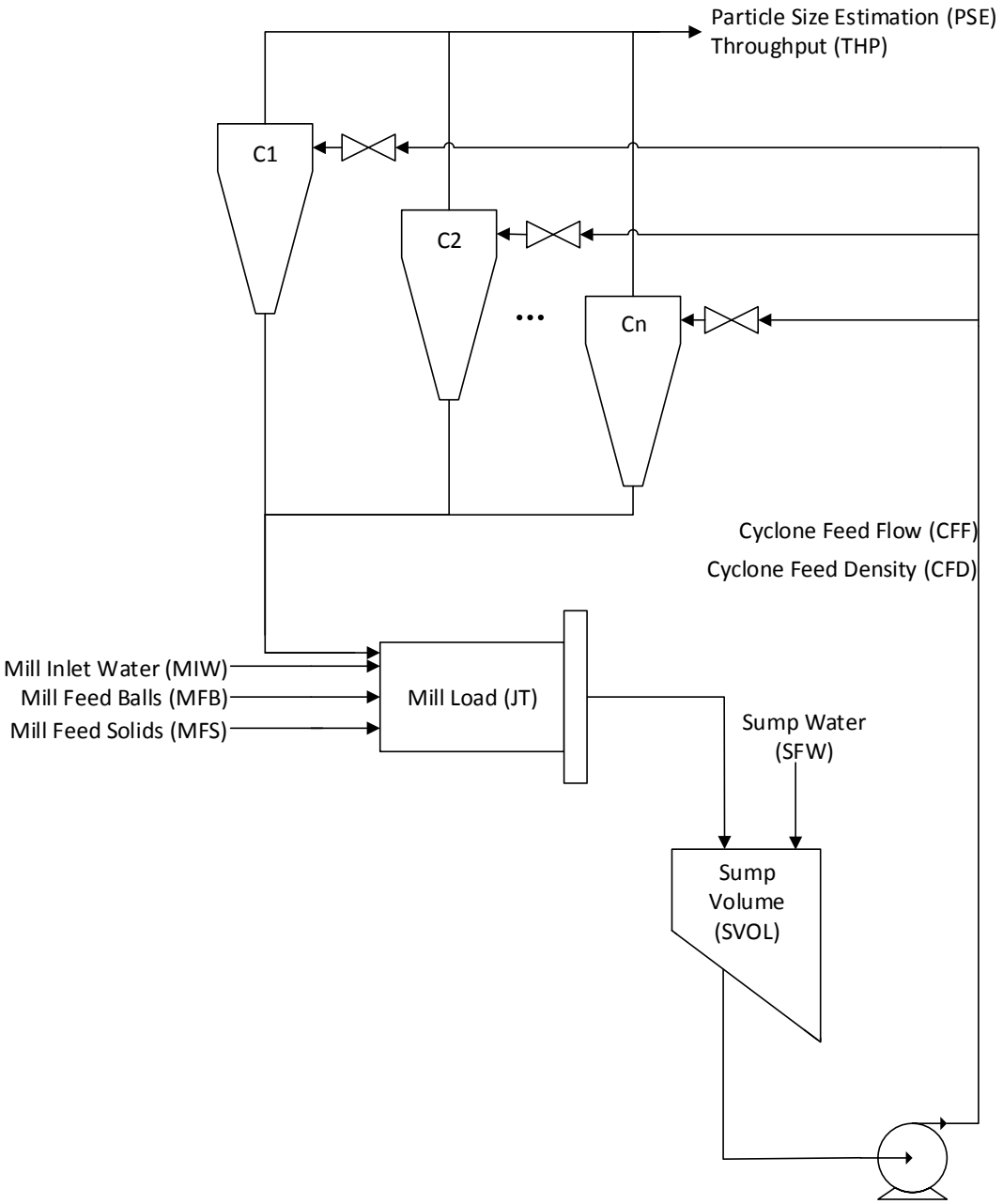

Figure 2.4. Single-stage grinding mill circuit with a hydrocyclone cluster.

2.3.2 Grinding mill circuit control

The norm for industrial milling circuit control is to use decoupled single-loop PID controllers, despite strong interactions between the loops [7].

The single-loop PID controllers are typically configured as follows:

- The load in the mill (J_T) is controlled by manipulated MFS.
- The volume in the sump is controlled by manipulating SFW.
- The product quality is controlled by manipulating. CFF
- The mill power draw with mill speed [7].

Since each CV is strongly coupled with all MVs, the decentralised PID control philosophy is prone to limiting the circuit performance. If one controller reaches a constraint and cannot maintain the process variable (PV) at setpoint, the other loops cannot attempt to offset the resulting setpoint error. In addition, the controllers simply maintain process stability while optimisation is left to the operator's discretion.

Maximising throughput while maintaining PSE at setpoint is desirable and is often achieved with real time optimisation strategies [22, 33].

In an attempt to achieve the optimal trade-off between the control objectives and integrate the optimisation objectives into the controllers, many multiple-input-multiple-output controllers have been developed [2, 6, 8, 9]. The supervisory fuzzy expert controller in [9] showed a 1.8% increase in throughput and a 2% reduction in power consumption for a SAG milling circuit when implemented, but was limited to a narrow operating region. A multivariable control framework was established for grinding mill circuits and subsequently a μ-synthesis controller was designed [23, 29]. The controller was implemented on an industrial plant and showed promise in controlling the mill load and product quality, but was not as promising in controlling the integrating sump level.

One of the most successful multivariable control techniques is model predictive control (MPC), which has been implemented to the extent that the term is used interchangeably with APC [34]. MPC was investigated as a possible multivariable control technique and showed promise, given the complexity of the grinding mill circuit [2, 8].

On top of the already complex nature of the grinding mill circuit, the circuit contains various non-linearities [1]. These non-linearities cause linear APC controllers, such as the MPC controllers in [2, 8], to be efficient in only narrow operating regions. These narrow operating regions are often large

enough for industrial operations, however some controller performance is lost and it will be beneficial to expand the operating region to always achieve maximum performance.

NMPC has an advantage over linear MPC, as the non-linearities can be captured in the model and the controller is efficient over a much wider operating region without compromising performance, since no linearisation is required [35]. This was proven by the RNMPC controller developed in [4]. The controller showed that even in the presence of large disturbances and model mismatch, it was possible to control a grinding mill circuit efficiently over an array of operating regions. The controller was however not practically viable, given the required controller execution time per iteration [4]. This drawback is becoming increasingly irrelevant owing to advances in processor performance leading to greatly reduced MPC algorithm execution times [34]. This technological improvement can be seen in [32], where a similar RNMPC controller was designed and simulated with sufficiently short execution times.

The grinding mill circuit is the first step in mineral comminution and therefore the economic benefit is not explicit. The controllers discussed so far have considered the grinding circuit in isolation, given static optimisation objectives. However, downstream process requirements play a critical role in the steady-state optimisation objective of the grinding mill circuit. Therefore in parallel to new control system developments for grinding mills, plantwide control strategies have been developed to improve the overall plantwide economic objective.

The key revenue-generating variable for the mineral processing plant is the concentrate grade and concentrate quantity of the downstream process (the separation circuit). In [36, 37] the product size distribution specification for the grinding mill circuit is continuously set by the separation circuit to improve the separation circuit's economic performance. An economic objective function is used in [38], where a predictive controller sets the targets for an advanced regulatory controller on the grinding circuit. The objective function optimised the income generated from the plant as a function of the feed ore grade relative to the grinding circuit, the separator tailings grade and the recovery of the plant.

The economic evaluation of a grinding mill circuit is done by using the relationship between the grinding mill circuit product particle size and the separation concentrate recovery and grade curve [25]. Economic plantwide optimisation for a mineral processing plant is therefore limited to the operating

range of the grinding mill circuit [39]. Grinding mill circuit controllers should be designed to optimise over a wide range of steady-state regions, incorporate various different CVs and MVs, and benefit from all dynamics in the circuit to reject upstream disturbances quickly to meet the plantwide economic objective.

In [40] a systematic procedure is given to find suitable MVs in order to construct a control architecture capable of achieving the plantwide economic optimisation objective. The MVs used to control the stability of the plant and those used to add functional controllability should be incorporated in the advanced controller. There should be enough MVs to independently control the CVs. Functional controllability refers to an optimisation objective such as reducing power or utility consumption or maximising throughput. To this end the robustness and operating regions of controllers can be improved by identifying additional MVs that can improve the functional controllability.

In [11] the range of quality control was increased by independently manipulating the mill's water feed rate instead of fixing the water feed rate as a ratio of the ROM ore feed rate. Similarly, in [12] the range of quality control was increased by manually switching hydrocyclones on top of an NMPC controller in a hydrocyclone cluster. Power consumption can be reduced while maintaining quality by alternating between different feed ore stockpiles and choosing whether a secondary grinding stage is used or not using linear HMPC [13]. In [14] and [15] the mill speed is used as an additional MV to reduce mill power consumption, and to control quality and throughput independently.

2.4 GRINDING MILL MODELLING AND STATE ESTIMATION

APC controllers require suitable process models that can be realistically fitted from process data and be updated with minimal process measurements. Grinding mill circuits have been modelled in various different ways. Because of the wide array of circuit topologies the circuit models should preferably be modular, where the mill, the sump and the classifier each has its own model [1].

2.4.1 Mill and sump modelling

Grinding mills have been modelled using linear transfer functions [2, 23, 29]. The transfer function matrix describes each circuit output given a certain input using either a first-order-plus-time-delay

model or an integrator with time-delay model. The models are derived using step test data.

Grinding mill circuits have also been modelled using neural networks [41]. Neural networks can easily capture the complex non-linearities in the grinding mill circuit from the input-output training data. However, the models are limited to the training data used and large data-sets are required. Therefore, in order to capture the effect of each disturbance and non-linearity, the process training data should contain multiple instances of each phenomenon.

The quality and throughput of mills can also be calculated from the mill speed and filling using grindcurves [10]. Grindcurves were used as the primary mill model in the RNMPC developed in [32].

Accurate models for SAG/AG mills can be described by a population mass balance. The Julius Kruttschnitt Mineral Research Centre developed a size-by-size solids mass balance model that has become a widely used model for simulating mills [42]. The model is a steady-state model typically used for mill design and has a large number of states and parameters, making it difficult to use for on-line applications [22]. A population mass balance model describes the accumulation of each size class within the mill and sump and takes the common form,

$$Accumulation = In - Out + Generation - Consumption. \tag{2.2}$$

The generation term describes the formation of smaller class particles and is a direct result of the breakage of ore. Similarly, for fines to be generated the ore is consumed and this relationship is contained in the consumption equation. (2.2) is also used for particles that cannot be consumed (for instance water), and the consumption/generation terms will be zero.

The phenomenological non-linear population balance model of [1] uses fewer parameters and states than [42] and [43], mainly by using fewer size classes to characterise the material in the circuit. This results in the model being practically viable in the use of APC controllers. Even with the reduced number of size classes, parameters and states, the model still gives qualitatively accurate results [44]. Because the model in [1] is modular, has reduced complexity, and has been proven qualitatively accurate, there are sufficient advantages in using this model for controller design over more complex simulation models.

2.4.2 Hydrocyclone modelling

The hydrocyclone in [1] is modelled as a set of static non-linear equations based on the Plitt hydrocyclone model. Hydrocyclones are typically modelled by using either the Plitt model or the Nageswararao model [22]. Commercial simulation software, JKSimMet, uses the Nageswararao model and is regarded as a reliable hydrocyclone model for mineral processing studies [45]. The Nageswararao model can accurately simulate a hydrocyclone over a large range of flow rates while allowing for the manipulation of various physical properties of the hydrocyclone. This is a potential drawback for industry application because it results in a large number of complex parameters that need to be estimated when compared to the Plitt model. The Plitt model uses energy efficiency curves to model the classifier, thereby reducing the number of model parameters [15, 46].

A comparison between the Nageswararao model and Plitt model was presented in [45]. The study concluded that if the parameters for the Plitt model are fitted to hydrocyclone data, the model is sufficient for industrial purposes when the operating point is close to the data obtained. [45] also concluded that the use of the Plitt model can be appropriate in simulations that do not use the JKSimMet simulation software, especially if the model is only used for control purposes with process feedback.

2.4.3 Milling circuit state estimation

Non-linear dynamic models are often implemented in state-space and require not only the plant input as a model input, but also the current model states. This is especially important considering that model-plant-mismatch will cause the actual plant states and the predicted states to differ [3]. The result is that in order to implement a non-linear model in an APC controller, a state estimator is required to estimate the model states, given the plant measurements [15].

This study focusses on the design of a new control scheme, and therefore certain assumptions are required about the measurements and peripheral control tools available when the controller is added to the control loop.

The extended Kalman filter has been used as a state estimator for mineral processing models [47, 48]. In [49] a neural network was trained on simulation data and used as a state estimator in the feedback

loop of an NMPC on a grinding mill circuit.

Particle filters do not require any training data and can be used with non-linear non-Gaussian systems. To benefit from these advantages a state and parameter estimator using dual particle filters was implemented in [50]. Similarly a fractional order disturbance observer as well as a Bode ideal cut-off disturbance observer for the grinding mill circuit was developed in [51].

Inferential based measurements have also been used to estimate the grinding mill product quality, ore quality and mill load [42, 52]. Although various state, parameter and disturbance estimators have been investigated for grinding mills, it remains a challenge to estimate mill hold-ups [15, 47].

2.5 HYBRID SYSTEMS

A grinding mill circuit, as shown in Figure 2.4, is often controlled by only considering the continuous dynamics, such as the continuous flow of ore, water or steel balls into the mill, the continuous mill speed, the continuous flow of water into the sump or slurry to the hydrocyclone. However, the grinding mill circuit has a number of discrete variables that can be controlled. Discrete variables are considered on/off variables. In the grinding mill circuit typical discrete components are conveyor belts that feed the circuit from different stockpiles, the number of active mills in a case where there are multiple mills in parallel, the use of a secondary grinding stage or the switching of hydrocyclones in a hydrocyclone cluster [16].

Models containing both discrete and continuous manipulated variables, such as the milling circuit represented in Figure 2.4, are referred to as hybrid systems. Hybrid systems are challenging to model, control and optimise [53].

A typical method of controlling hybrid systems is using a layered approach, where the bottom layer controls the continuous plant input variables, and the top layer controls the discrete dynamics (typically according to some optimisation function) [54]. This can be seen in milling circuits with a bottom layer controlling the continuous dynamics of the mill, sump, and hydrocyclone feed, and a top layer controlling the switching of individual hydrocyclones in the cluster [18].

It is not always easy to distinguish between the layers in a grinding mill circuit. If there are multiple mills in parallel, the supervisory controller might opt to switch one mill off; however, this will result in a loss of circuit throughput. The end result will be economically less viable than if there had been only continuous controllers. Similarly, the optimal number of hydrocyclones to use in a cluster of hydrocyclones depends on the circulating load and the hardness of the mill feed ore. Therefore, to consider simply the hydrocyclone cluster feed pressure or feed flow to switch hydrocyclones will not result in optimal economic benefit, and often leads to unnecessary hydrocyclone switching. An APC controller can therefore greatly benefit from incorporating the continuous and switching dynamics in the circuit to ensure optimal operation of the process [19, 55, 56].

Hybrid models are often modelled as mixed logical dynamical (MLD) models [53, 19]. An MLD model combines the linear dynamic equations, continuous and discrete input variables and states with linear inequalities to contain the constraints. From [57] an MLD model takes the form of

$$x(k+1) = Ax(k) + B_1u(k) + B_2\delta(k) + B_3z(k), \tag{2.3a}$$

$$y(k) = Cx(k) + D_1u(k) + D_2\delta(k) + D_3z(k), \tag{2.3b}$$

$$E_1x(k) + E_2u(k) + E_3\delta(k) + E_4z(k) \leq g_5, \tag{2.3c}$$

where $x(k) = [x_r(k), x_b(k)]$ is a matrix consisting of the vectors $x_r(k) \in \mathbb{R}$ and $x_b(k) \in \{1,0\}$; $y(k) = [y_r(k), y_b(k)]$ is a matrix consisting of the vectors $y_r(k) \in \mathbb{R}$ and $y_b(k) \in \{1,0\}$; $u(k) = [u_r(k), u_b(k)]$ is a matrix consisting of the vectors $u_r(k) \in \mathbb{R}$ and $u_b(k) \in \{1,0\}$, and where $z(k) \in \mathbb{R}$ and $\delta(k) \in \{1,0\}$ are vectors of auxiliary variables. The MLD form in (2.3) describes a hybrid system by explicitly combining the linear continuous dynamics and discrete components. The discrete process input variables or state descriptions do not have to be contained in the A or B matrix but can be added as auxiliary variables [57].

2.6 ADVANCED PROCESS CONTROL METHODS

2.6.1 Non-linear model predictive control

MPC is a control technique in which optimal control is applied in an iterative fashion [35]. The control problem is solved at each iteration based on the plant measurements, predicted states, and the past predictive move pattern. An MPC controller is also referred to as a receding horizon controller. At

each iteration the controller will observe the past control moves, the current plant condition (based on the measurements) and the desired operating point (CV setpoints and optimisation objective trajectory). The controller will then predict the plant outputs (according to some plant model and the estimated model states from the plant measurements) over a prediction horizon given a vector of MVs (control moves). During the iteration an optimiser will estimate the optimal control moves that drive the process to the desired setpoints according to some objective function based on the predicted plant outputs. Once the optimal control move vector has been calculated, only the first move is implemented and the process is repeated [58]. NMPC follows the same principle of operation as a linear MPC, except that a non-linear model is used to predict the plant outputs and the solver or optimiser should be able to cope with possible local optimums and non-linear models. The block diagram in Figure 2.5 illustrates the NMPC principle of operation as discussed. In Figure 2.5 u is the controller output applied to the process when the controller converged to a solution, while $u_{predicted}$ is the continuously changing matrix of control moves that the controller estimates over the control horizon to drive the process to the desired operating condition. When the controller achieves a feasible solution u is the first vector of control moves in $u_{predicted}$.

MPC has become increasingly popular (especially in grinding mill circuits as seen in Section 2.3.2) because:

- the objective function is flexible and can contain setpoint control, buffer control, optimisation objectives, and penalise large control moves,
- equality and inequality constraints can be added directly to the controller ensuring feasible control moves at all times,
- virtually any type of process model can be used (although the more complex the model, the longer the controller execution time will be),
- the controller is inherently multivariable and priorities on CVs and MVs can easily be adjusted in the objective function, and
- the controller has good disturbance rejection as it is inherently feed forward [35, 58].

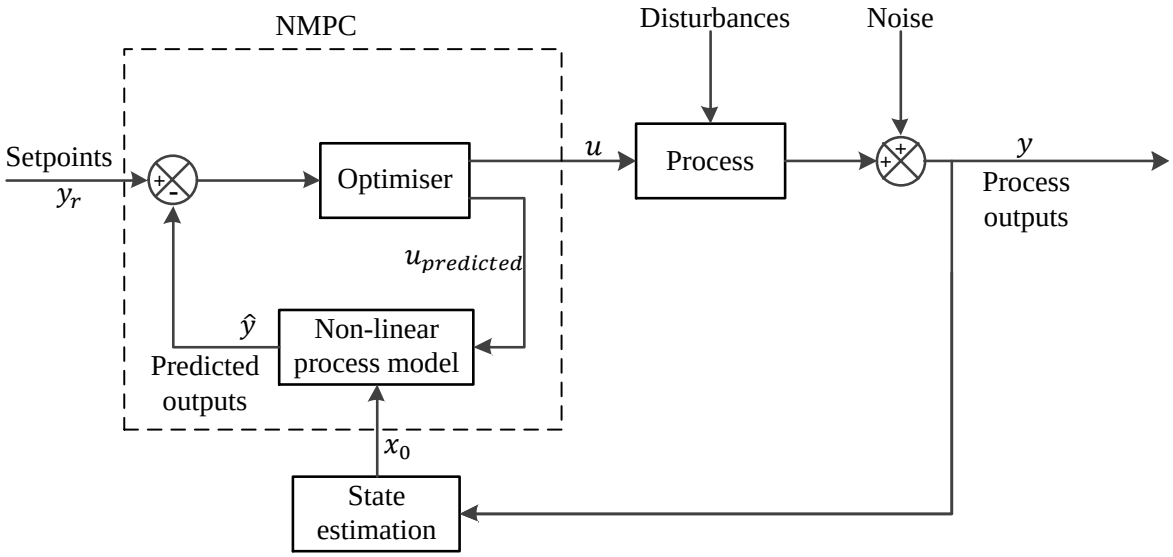

Figure 2.5. Non-linear model predictive control.

2.6.2 Hybrid non-linear model predictive control

As discussed in Section 2.5, the discrete and continuous dynamics in hybrid systems are strongly coupled, and as such APC controllers could achieve additional benefits by considering both discrete and continuous dynamics as part of the optimal control solution. HMPC has shown promise in controlling hybrid systems by predicting, controlling and utilising the continuous and discrete-time process variables and process inputs.

Special software packages such as HYSDEL can automatically convert linear hybrid models to MLD models [59]. The objective function can then be formulated into a set of linear inequalities and mixed integer quadratic programming is then used as the optimisation engine [56, 59]. The combination of the linear inequalities and the process model forms the HMPC control strategy [53]. This method was applied to grinding mill circuits where the hybrid controller could select which ore stock pile to feed from, or which grinding stage should be active [13]. The control framework for HMPC of grinding mill circuits in [21] follows the same methodology.

HMPC controllers can also be implemented to follow a more direct approach. The HMPC controller formulation will be similar to that of an NMPC (as discussed in Section 2.6.1), but the model will be

the hybrid model and the solver must be able to solve mixed-integer problems. This approach was followed in [19] where the system was modelled using MLD, but the solver was a modified particle swarm optimisation (MPSO) algorithm.

However, in the grinding mill literature presented so far, it is evident that the non-linearities in the grinding mill circuit have a large influence on the control objective. The benefits of NMPC over conventional control methods were discussed in Section 2.3.2. Similarly, in Section 2.5 it was shown that the grinding mill circuit has various discrete inputs that should be considered by the APC controller. Some of the benefits of incorporating the discrete dynamics were illustrated in [12], where the range of operability of an NMPC was increased by manually switching hydrocyclones in a grinding mill circuit. Therefore, an HMPC controller for a grinding mill circuit should not just incorporate the discrete and continuous dynamics, but should also be able to use non-linear models.

Hybrid non-linear model predictive control (HNMPC) was implemented in [20] where the non-linear hybrid model was implemented directly and a genetic algorithm (GA) was used as an optimiser. This type of non-linear hybrid controller has yet to be implemented on grinding mill circuits. Based on the advantages gained in grinding mill circuit performance from NMPC controllers and the switching of discrete dynamics, and the requirements of APC controllers stemming from plantwide control, HNMPC should be considered.

2.6.2.1 Genetic algorithm

The GA calculates an initial set of solutions (for all the input variables) called the population. The population aims to minimise the GA fitness function (which is a a performance function supplied to evaluate the fit of each solution in the population) within constraints. The first GA iteration is the initial “guess” given to the GA algorithm. The GA generates a new population through recombination or crossover combined with a stochastic mutation function of the best fit variable sets in the population. The new population is referred to as the next generation. The mutation function uses the best fit variable values in the population and then discards the other variable values and defines new values based on a stochastic function. The process is repeated until the minimum fitness function value is reached, or the maximum number of generations is exceeded [60].

The GA has advantages over other mixed-integer solvers such as MPSO because of the following:

- It is able to solve problems with strong non-linearities - the MPSO had to be altered in order to handle non-linearities [61].
- Because of the stochastic nature of the solver, it can accommodate large variations in the initial "guess" input (if there is an initial input).
- The stochastic nature of the solver also ensures a global minimum in the presence of many local minima.
- The solver can handle hard constraints on inputs, outputs and model states.
- The solver can handle large sets of mixed-integer inputs without an effect on solver performance [20, 62].

These advantages motivate the GA as a suitable solver for HNMPC and it is used as the optimiser in the HNMPC formulated in Section 4.4.

2.7 CONCLUSION

In this chapter a body of knowledge regarding grinding mill circuits was given. The body of knowledge consisted of an overview of the grinding mill circuit, its operating philosophy, a brief history of controllers implemented on the circuit and the way in which the circuit is modelled for control purposes.

In Section 2.4.1 a non-linear continuous time grinding mill circuit model was identified. The model is modular and presented in Chapter 3, where it is expanded and some parameters are refitted so that the model has a cluster of hydrocyclones instead of just one hydrocyclone.

The expansion of the model as done in Chapter 3 is required, since it has been shown that for hybrid systems, it is important to incorporate the discrete components of a circuit into the controller formulation. HMPC has shown promise in controlling hybrid systems, and has even been implemented on grinding mill circuits. However, a gap was identified in the literature, as the HMPC controllers for grinding mill circuits only considered linear dynamics for the continuous part of the model. The

advantages of NMPC have been shown for grinding mill circuits, and although HNMPC has been formulated and applied to other processes, it has not been done for a grinding mill circuit.

CHAPTER 3 HYBRID MODEL OF A SINGLE-STAGE GRINDING MILL CIRCUIT WITH A HYDROCYCLONE CLUSTER

3.1 CHAPTER OVERVIEW

In this chapter the dynamic phenomenological non-linear population balance model of [1] is discussed in detail with all the associated states, inputs, outputs and parameters. The mill, sump and hydrocyclone are modelled separately and the hydrocyclone model is expanded to describe a cluster of hydrocyclones such that a non-linear hybrid model explicitly containing continuous and discrete dynamics is created. The hydrocyclone parameters in [1] had to be re-fitted to accommodate a hydrocyclone cluster. The model presented in this chapter is used in the formulation of the NMPC and HNMPC controllers in Chapter 4. The model is also used in Chapter 5 as the simulation model.

3.2 MODEL OVERVIEW AND NOMENCLATURE

As discussed in Section 2.4.1, the model in [1] uses fewer parameters and states for the mill and hydrocyclone than [43] and [42] by using fewer size classes to characterise the material in the circuit. The model is still qualitatively accurate despite the reduced number of size classes [44].

The model uses three size classes to describe the material in the circuit: rocks, coarse ore and fine ore:

- Ore in the mill that is too large to pass through the end-discharge screen are referred to as rocks.

- Particles discharged through the end-discharge screen larger than the specification size are referred to as coarse particles.
- Particles discharged through the end-discharge screen, which are within the specification size, are referred to as fines.

The manipulated, measured and controlled variables commonly used in industry for a grinding mill circuit are shown in Table 3.1 [7].

Table 3.2 gives a description of each symbol and its respective subscripts used in the model. In Table 3.2 the variable V denotes volumetric flow rates in m^3/h and X denotes the states of the model as volume of material in m^3. The first subscript indicates the process unit (mill, sump, cyclone), the second subscript specifies the state (water, balls, rocks, solids, fines), and in the case of flow rates the third subscript indicates an inflow, outflow, or underflow.

The nomenclature for the mill and sump model is given in Table 3.3, and the nomenclature for the hydrocyclone in Table 3.4. The parameter values for the mill and sump were taken from [1], and the parameter values for the hydrocyclone cluster were refitted based on the data in [1].

3.3 MILL MODEL

The SAG mill is modelled using a mass balance approach by incorporating the effects of mill power draw and slurry rheology in the calculation of the mill load and breakage power functions. The constituents of charge in the mill are represented by five states: rocks (X_{mr}), solids (X_{ms}), fines (X_{mf}), balls (X_{mb}) and water (X_{mw}). It is important to note that although there are three size classes, the model does not have a model state for coarse material, but rather one for solids. The choice not to model coarse ore but rather solids simplify the modelling of the mill and the sump. The model describes the states by considering the inflow, outflow, generation and consumption of each state. Solids are the summation of fines and coarse particles.

Table 3.1. Grinding mill circuit variables

Variable	Description	Unit
Manipulated Variables		
MIW	Flow rate of water to the mill	[m^3/h]
MFS	Feed rate of ore to the mill	[t/h]
MFB	Feed rate of steel balls to the mill	[t/h]
SFW	Flow rate of water to the sump	[m^3/h]
CFF	Flow rate of slurry to the hydrocyclone cluster	[m^3/h]
Controlled Variables		
J_T	Fraction of the mill volume filled with charge	[-]
$SVOL$	Volume of slurry in sump	[m^3]
PSE	Product particle size estimate	[-]
Measured Variables		
P_{mill}	Power draw of the mill motor	[kW]
THP	Throughput	[t/h]
CFD	Hydrocyclone feed density	[t/m^3]

The state equations describing the dynamics of the mill hold-ups are,

$$\dot{X}_{mw} = V_{mwi} - V_{mwo} + V_{cwu} \tag{3.1a}$$

$$\dot{X}_{ms} = V_{msi} - V_{mso} + V_{csu} + RC \tag{3.1b}$$

$$\dot{X}_{mf} = V_{mfi} - V_{mfo} + V_{cfu} + FP \tag{3.1c}$$

$$\dot{X}_{mr} = V_{mri} - RC \tag{3.1d}$$

$$\dot{X}_{mb} = V_{mbi} - BC \tag{3.1e}$$

where V_{mwi}, V_{msi}, V_{mfi}, V_{mri}, and V_{mbi} (m^3/h) are the feed rates of water, solids, fines, rocks and balls into the mill respectively; V_{cwu}, V_{csu}, and V_{cfu} (m^3/h) are the flow-rates of the water, solids and fines at the underflow of the hydrocyclone cluster respectively; V_{mwo}, V_{mso}, and V_{mfo} (m^3/h) are the flow rates of water, solids and fines from the mill to the sump respectively. RC, FP, and BC (m^3/h) represent rock consumption, fines production and ball consumption respectively and are given in (3.5), (3.6) and (3.7).

Table 3.2. Description of subscripts

Subscript	Description
$X\square_{-}$	m-mill; s-sump; c-hydrocyclone cluster; cj-jth hydrocyclone
$X_{-}\square$	w-water; s-solids; c-coarse; f-fines; r-rocks; b-balls
$V_{--}\square$	i-inflow; o-outflow; u-underflow

Table 3.3. Mill model parameters from [1]

Parameter	Value	Description
α_f	0.055	Fraction of fines in the feed ore
α_r	0.465	Fraction of rocks in the feed ore
α_P	1.0	Fractional power reduction per fractional reduction from maximum mill speed
α_{ϕ_f}	0.01	Fractional change in kW/t fines produced per change in fractional filling of mill
α_{speed}	0.72	Fraction of critical mill speed
δ_{P_s}	17.46	Power-change parameter for fraction of solids in the mill
δ_{P_v}	17.46	Power-change parameter for volume of mill filled
D_B	7.85	Density of steel balls [t/m^3]
D_S	3.2	Density of feed ore [t/m^3]
ε_{sv}	0.6	Maximum fraction of solids by volume of slurry at zero slurry flow
ϕ_b	90.0	Steel abrasion factor [kWh/t]
ϕ_f	29.5	Power needed per tonne of fines produced [kWh/t]
ϕ_r	6.72	Rock abrasion factor [kWh/t]
$\varphi_{P_{max}}$	0.57	Rheology factor for maximum mill power draw
P_{max}	1670	Maximum mill motor power draw [kW]
v_{mill}	59.12	Mill volume [m^3]
$v_{P_{max}}$	0.34	Fraction of mill volume filled for maximum power draw
V_V	88.0	Volumetric flow per “flowing volume” driving force [h^{-1}]

ROM ore, additional water and steel balls are fed into the mill and the mill input streams are described as,

$$V_{mwi} = MIW \tag{3.2a}$$

$$V_{msi} = \frac{MFS}{D_S}(1-\alpha_r) \tag{3.2b}$$

$$V_{mfi} = \frac{MFS}{D_S}\alpha_f \tag{3.2c}$$

$$V_{mri} = \frac{MFS}{D_S}\alpha_r \tag{3.2d}$$

$$V_{mbi} = \frac{MFB}{D_B}, \tag{3.2e}$$

where MIW (m^3/h) is the mill flow rate of water, MFS (t/h) is the feed rate of ROM ore into the mill and MFB (t/h) is the feed rate of steel balls into the mill; D_S and D_B (t/m^3) are the feed ore and steel ball densities respectively; α_f and α_r represent the fraction of fines and rocks in MFS respectively.

Material discharge flow rates from the mill to the sump are calculated as,

$$V_{mwo} = V_V \varphi X_{mw} \frac{X_{mw}}{X_{ms}+X_{mw}} \tag{3.3a}$$

$$V_{mso} = V_V \varphi X_{mw} \frac{X_{ms}}{X_{ms}+X_{mw}} \tag{3.3b}$$

$$V_{mfo} = V_V \varphi X_{mw} \frac{X_{mf}}{X_{ms}+X_{mw}} \tag{3.3c}$$

where V_V $(1/\text{h})$ is the volumetric fractional discharge rate and φ is an empirical function called the rheology factor. Parameter V_V accounts for the shape and build of the end-discharge screen.

Rheology describes the behaviour of non-Newtonian fluids (such as the slurry of ground ore and water). The rheology factor therefore incorporates the effect of the fluidity and density of the slurry in the calculation of the milling circuit's performance [63]. This relationship is shown in Figure 3.1 where the effect of the ratio between the mill solids and water on the rheology is shown. A rheology factor of one will indicate the slurry is non-flowing, while a rheology factor of zero is the result of no solids in the slurry and is therefore only water. The rheology factor is calculated as,

$$\varphi = \left(\max\left[0, \left(1-\left(\frac{1}{\varepsilon_{sv}}-1\right)\frac{X_{ms}}{X_{mw}}\right)\right]\right)^{0.5} \tag{3.4}$$

where ε_{sv} is the fraction of solids in the slurry that will result in no flow.

The material consumption and generation equations are,

$$RC = \frac{P_{mill}\varphi}{D_S \phi_r}\left(\frac{X_{mr}}{X_{mr}+X_{ms}}\right) \tag{3.5}$$

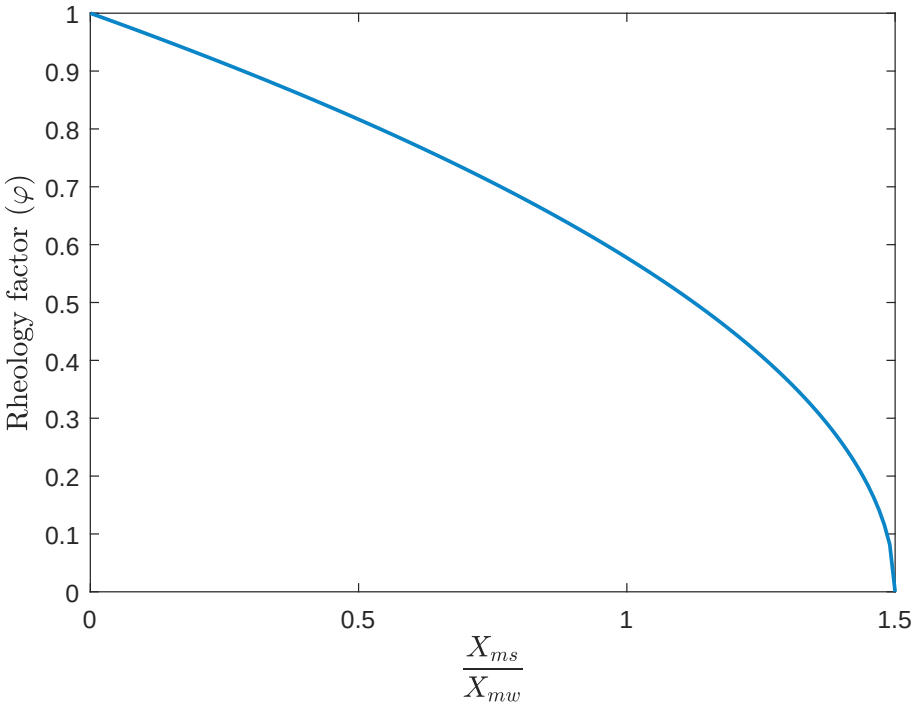

Figure 3.1. Rheology factor as a function of the ratio of solids to water in the mill.

$$FP = \frac{P_{mill}}{D_S \phi_f}\left[1+\alpha_{\phi_f}\left(\frac{X_{mw}+X_{mr}+X_{ms}+X_{mb}}{v_{mill}} - v_{P_{max}}\right)\right]^{-1} \tag{3.6}$$

$$BC = \frac{P_{mill}\varphi}{\phi_b}\left(\frac{X_{mb}}{D_S(X_{mr}+X_{ms})+D_B X_{mb}}\right) \tag{3.7}$$

where P_{mill} (kW) is the power draw of the mill, ϕ_b and ϕ_r (kWh/t) are the ball and rock abrasion factors respectively, ϕ_f (kWh/t) is the power needed per tonne of fines produced, α_{ϕ_f} is the fractional change in ϕ_f as a result of the mill filling and $v_{P_{max}}$ is the mill load for maximum power draw.

3.3.1 Mill measured variables

There are two common measured variables for the mill: the mill load and the mill power draw. The fraction of the mill filled can be related to the mill load and is a critical CV to ensure steady operation of the grinding mill circuit and to reduce downtime by avoiding unnecessary mill liner wear. The fraction of the mill filled is calculated as,

$$J_T = \frac{X_{mw}+X_{ms}+X_{mr}+X_{mb}}{v_{mill}} \tag{3.8}$$

where v_{mill} (m^3) is the volumetric size of the mill. The power draw of the mill is defined as,

$$P_{mill} = P_{max}\{1-\delta_{Pv}Z_x^2 - 2\chi_P\delta_{Pv}\delta_{Ps}Z_xZ_r - \delta_{Ps}Z_r^2\}\cdot(\alpha_{speed})^{\alpha_P} \tag{3.9}$$

where P_{max} (kW) is the maximum mill power draw, α_{speed} is the fraction of critical mill speed, α_P is the fractional change in mill power draw due to a change in α_{speed}; δ_{Pv} and δ_{Ps} are parameters estimating power draw change due to the volume of the mill filled and fraction of solids in the mill respectively. The effect of the total charge on mill power is modelled by the empirical function

$$Z_x = \frac{J_T}{\varphi_{P_{max}}} - 1, \tag{3.10}$$

and the effect of the solids content on the mill power is modelled by the empirical function

$$Z_r = \frac{\varphi}{\varphi_{P_{max}}} - 1, \tag{3.11}$$

where $\varphi_{P_{max}}$ is the rheology factor at maximum mill power draw.

3.4 SUMP MODEL

Because of the end-discharge screen of the mill, which prevents rocks and balls from exiting the mill, the sump will not contain any steel balls or rocks. The sump states are therefore water (X_{sw}), solids (X_{ss}), and fines (X_{sf}). The dynamics of the sump hold-ups are governed by the following state equations,

$$\dot{X}_{sw} = V_{mwo} - V_{swo} + SFW \tag{3.12a}$$

$$\dot{X}_{ss} = V_{mso} - V_{sso} \tag{3.12b}$$

$$\dot{X}_{sf} = V_{mfo} - V_{sfo}, \tag{3.12c}$$

where V_{swo}, V_{sso} and V_{sfo} (m^3/h) are the sump discharge flow-rates of water, solids and fines respectively. It is assumed that the constituents in the sump are fully mixed. The discharge of each state from the sump through the variable speed pump is defined as,

$$V_{swo} = CFF\frac{X_{sw}}{X_{sw}+X_{ss}} \tag{3.13a}$$

$$V_{sso} = CFF\frac{X_{ss}}{X_{sw}+X_{ss}} \tag{3.13b}$$

$$V_{sfo} = CFF\frac{X_{sf}}{X_{sw}+X_{ss}}. \tag{3.13c}$$

The sump volume, which is related to sump level, $SVOL$ (m^3), is a critical CV. A controller should ensure that the sump does not run dry or overflows. The hydrocyclone cluster feed density, CFD (t/m^3), is controlled by manipulating the flow of water to the slurry in the sump, SFW (m^3/h). In this study, CFD is not directly controlled, but where possible it should be minimised in order to maximise the circulating load and increase the classifier performance [32]. Therefore, even though CFD is not

directly controlled, it should be monitored in the simulation study. From the sump model the variables $SVOL$ and CFD can be calculated as,

$$SVOL = X_{ss} + X_{sw} \tag{3.14a}$$

$$CFD = \frac{X_{sw} + X_{ss} D_s}{X_{sw} + X_{ss}}. \tag{3.14b}$$

3.5 HYDROCYCLONE CLUSTER MODEL AND REFITTING OF PARAMETERS

As discussed in Section 2.5, a hybrid model is a model that incorporates continuous and discrete time dynamics [59]. So far this chapter has only discussed continuous time dynamics for the grinding mill circuit. The SAG mill model and the sump only had continuous states and process inputs.

This section will give the continuous dynamics of each individual hydrocyclone, but also introduce discrete input variables that represent the switching in and out of individual hydrocyclones in the hydrocyclone cluster. With the expansion of the hydrocyclone model to a hydrocyclone cluster model it is important to note the following:

- The hydrocyclone cluster should contain a realistic number of hydrocyclones (as close to a practical implementation as possible) but the number should also allow for realistic switching dynamics, i.e. provide enough resolution. For example, if only two hydrocyclones are in the cluster, the switching will have a huge effect on the operating condition and the move will outweigh all other CVs. Therefore one switching event should have a comparable effect to the other CVs to ensure that HNMPC is viable.
- With the sizing of the cluster the nominal number of active hydrocyclones should achieve exactly the same steady-state conditions as if only one hydrocyclone had been used. This is to ensure the mass balance around the mill and sump and to maintain a similar circulating load in order to ensure the integrity of the mill and sump models.

It was shown that in a grinding mill circuit where the feed ore hardness and particle size distribution experience sporadic changes, the number of required active hydrocyclones changes quite significantly [17]. In line with the approach taken in [17], the hydrocyclone in [1] should be replaced with a cluster of nine hydrocyclones of which eight are active under nominal operating conditions. This choice will allow for the inclusion of hydrocyclone switching as an additional CV. Switching one hydrocyclone

in the cluster has a similar effect to changing CFF by 11% if only one hydrocyclone is present. A minimum of six hydrocyclones must always be active to ensure process stability and simulate a real world environment [18]. The individual hydrocyclone parameters were refitted in this study to produce similar steady-state results as in [1]. This is also the number of hydrocyclones chosen in the paper published from this work [12].

As discussed in Section 2.5, hybrid systems are commonly modelled as MLD models. This study follows a more direct approach in that the model is not linearised and all non-linear equations are used as is. Similarly, the discrete variables are added directly to the model as a switching vector containing only discrete variables. This more direct approach to implementing the discrete inputs requires the inputs to be added as auxiliary variables rather than forming part of the continuous input vector [57]. The common form for an MLD model containing linear dynamics can then be altered to a non-linear common form with the discrete activation variables,

$$\begin{aligned} \dot{\mathbf{x}} = &\quad \mathbf{f}(t,\mathbf{x},\mathbf{u},\rho) \\ \mathbf{y} = &\quad \mathbf{h}(t,\mathbf{x},\rho) \\ &with \\ \mathbf{x} &\quad \in \mathbb{R} \\ \mathbf{u} &\quad \in \mathbb{R} \\ \mathbf{y} &\quad \in \mathbb{R} \\ \rho &\quad \in \{1,0\}, \end{aligned} \tag{3.15}$$

where $\mathbf{x}$, $\mathbf{y}$, and $\mathbf{u}$ represent the plant's state, measured variables, and MVs respectively. The vector of activation signals for the individual hydrocyclones in the cluster is ρ. The variables for the complete continuous non-linear model for the grinding mill circuit are given by,

$$\mathbf{x} = [X_{mw}, X_{ms}, X_{mf}, X_{mr}, X_{mb}, X_{sw}, X_{ss}, X_{sf}]^T \tag{3.16a}$$

$$\mathbf{u} = [MFS, MIW, MFB, SFW, CFF]^T \tag{3.16b}$$

$$\mathbf{y} = [J_T, P_{mill}, SVOL, CFD, PSE, THP]^T. \tag{3.16c}$$

The functions containing the non-linear hybrid dynamics are contained in $\mathbf{f}$, which is given in (3.1) and (3.12), and $\mathbf{h}$, which is given in (3.8), (3.9), (3.14), and (3.22). The vector ρ consists of the activation variables for each hydrocyclone, ρ_j, where j is used to indicate a specific hydrocyclone,

$$\rho_j = \begin{cases} 1 & \text{if hydroyclone ON} \\ 0 & \text{if hydrocyclone OFF} \end{cases} \tag{3.17}$$
$$j = 1,2,3...,N_{cyclones},$$

where $N_{cyclones}$ is the total number of hydrocyclones in the cluster. The number of active cyclones in the cluster is defined as,

$$N_{ActiveCyclones} = \sum_{j=1}^{N_{cyclones}} \rho_j. \tag{3.18}$$

The hydrocyclone modelled in [1] is represented as a set of static non-linear volumetric flow rate equations based on the Plitt hydrocyclone model. The product size and density are modelled by taking the slurry density, slurry viscosity, and the effects of angular velocity of the particles inside the hydrocyclone into account. Identical hydrocyclones are used in the cluster and the parameters for each hydrocyclone will therefore be the same.

The flow rate at the underflow of the j-th hydrocyclone can be calculated from,

$$CFF_j = \frac{CFF}{N_{ActiveCyclones}} \tag{3.19a}$$

$$V_{cjcu} = \rho_j \frac{CFF_j\,(X_{ss} - X_{sf})}{X_{sw} + X_{ss}} \left(1 - C_1 \exp\left(\frac{-CFF_j}{\varepsilon_c}\right)\right) \left(1 - \left(\frac{F_i}{C_2}\right)^{C_3}\right) \left(1 - P_i^{C_4}\right) \tag{3.19b}$$

$$V_{cjwu} = \rho_j \frac{X_{sw}\,(V_{cjcu} - F_{uj} V_{cjcu})}{F_{uj} X_{sw} + F_{uj} X_{sf} - X_{sf}} \tag{3.19c}$$

$$V_{cjfu} = \rho_j \frac{X_{sf}\,(V_{cjcu} - F_{uj} V_{cjcu})}{F_{uj} X_{sw} + F_{uj} X_{sf} - X_{sf}} \tag{3.19d}$$

$$V_{cjsu} = V_{cjcu} + \rho_j \frac{X_{sf}\,(V_{cjcu} - F_{uj} V_{cjcu})}{F_{uj} X_{sw} + F_{uj} X_{sf} - X_{sf}} \tag{3.19e}$$

where CFF_j (m^3/h) refers to the hydrocyclone feed for each individual hydrocyclone; V_{cjcu}, V_{cjwu},V_{cjfu}, and V_{cjsu} (m^3/h) are the underflow of coarse ore, water, fines and solids for the j-th hydrocyclone respectively; $F_i = V_{sso}/CFF$ is the fraction of solids in the hydrocyclone cluster feed; $P_i = V_{sfo}/V_{sso}$ is the fraction of fines in the feed solids; ε_c (m^3/h) relates to the coarse split; C_1 relates to the split at low-flows when the centrifugal force on particles is small; C_2 normalises the fraction of solids in the feed according to the maximum packing fraction of solid particles and C_3 and C_4 adjusts the sharpness of the dependency on F_i and P_i. The fraction of solids in the underflow volume for each hydrocyclone is,

$$F_{uj} = 0.6 - \left(0.6 - \frac{X_{ss}}{X_{sw}+X_{ss}}\right) \exp\left(\frac{-V_{cjcu}}{\alpha_{su}\varepsilon_c}\right) \tag{3.20}$$

where α_{su} relates to the fraction of solids in the underflow.

The total underflow recycled to the mill is the summation of all the underflow streams. The flow rates at the overflow of each hydrocyclone are,

$$V_{cjso} = \rho_j \frac{CFF_j X_{ss}}{X_{ss} + X_{sw}} + \rho_j \frac{X_{sf}\left(V_{cjcu} - F_{uj} V_{cjcu}\right)}{F_{uj} X_{sw} + F_{uj} X_{sf} - X_{sf}} - V_{cjcu} \tag{3.21a}$$

$$V_{cjfo} = \rho_j \frac{CFF_j X_{sf}}{X_{ss} + X_{sw}} - \rho_j \frac{X_{sf}\left(V_{cjcu} - F_{uj} V_{cjcu}\right)}{F_{uj} X_{sw} + F_{uj} X_{sf} - X_{sf}} \tag{3.21b}$$

$$V_{cjwo} = \rho_j \frac{CFF_j X_{sw}}{X_{ss} + X_{sw}} - V_{cjwu}. \tag{3.21c}$$

The total overflow of solids, fines and water for the hydrocyclone cluster is the summation of all the individual overflows of solids, fines and water. The grinding mill circuit throughput (THP) and quality (PSE) are calculated as,

$$V_{cfo} = \sum_{j=1}^{N_{cyclones}} V_{cjfo} \tag{3.22a}$$

$$V_{cso} = \sum_{j=1}^{N_{cyclones}} V_{cjso} \tag{3.22b}$$

$$PSE = \frac{V_{cfo}}{V_{cso}} \tag{3.22c}$$

$$THP = V_{cso} D_s, \tag{3.22d}$$

where V_{cfo} and V_{cso} (m^3/h) are the overflow flow rates of fines and solids respectively for the cluster as a whole.

In this study the single hydrocyclone in [1] is replaced with a cluster of nine hydrocyclones, with a nominal operating value of eight hydrocyclones. A minimum of six cyclones must always be active. The individual hydrocyclone parameters were refitted in this study to produce similar steady-state results as in [1].

3.5.1 Refitting of hydrocyclone parameters for a cluster

In [1] steady-state process data for the grinding mill circuit were used to fit the model parameters. To use the model parameters from [1], the discharge rates of the mill, sump and hydrocyclone cluster in this study should conform to the given ranges. The circuit considered in this study has a hydrocyclone cluster with nine cyclones, with a nominal operating value of eight hydrocyclones. Therefore, if the single hydrocyclone in [1] is replaced with a cluster with eight active hydrocyclones, the individual

hydrocyclone parameters need to be refitted for the hydrocyclone cluster to achieve exactly the same throughput and quality of [1] given the same feed streams.

As discussed, the individual hydrocyclone parameters are α_{su}, C_1, C_2, C_3, C_4, and ε_c. All of these parameters, except ε_c, are dimensionless and a change in the nominal operating flow of the hydrocyclone will not influence the parameters, therefore none of them has to be changed. Only ε_c (m^3/h) needs to be altered to achieve the same course split at a lower nominal flow rate per hydrocyclone.

ε_c was calculated using the equation relating the coarse split to the hydrocyclone feed, given by

$$\frac{V_{ccu}}{V_{cci}} = 1 - C_1 e^{\frac{-CFF}{\varepsilon_c}}. \tag{3.23}$$

With $C_1 = 0.6$, the nominal flow rate of the hydrocyclone CFF = 374 m^3/h, and ε_c = 129 m^3/h, the coarse split for the survey data in [1] was calculated as,

$$\frac{V_{ccu}}{V_{cci}} = 0.967. \tag{3.24}$$

With the cluster (and eight active hydrocyclones) the nominal flow rate over each hydrocyclone becomes $CFF_j = 46.75$ m^3/h. Therefore to achieve the same course split at the new nominal flow, ε_c was calculated using (3.23), resulting in,

$$\varepsilon_c = 15.867 m^3/h. \tag{3.25}$$

Figure 3.2 shows that the smaller hydrocyclone has the same course split (given a lower CFF value) than the original hydrocyclone (with its higher CFF value).

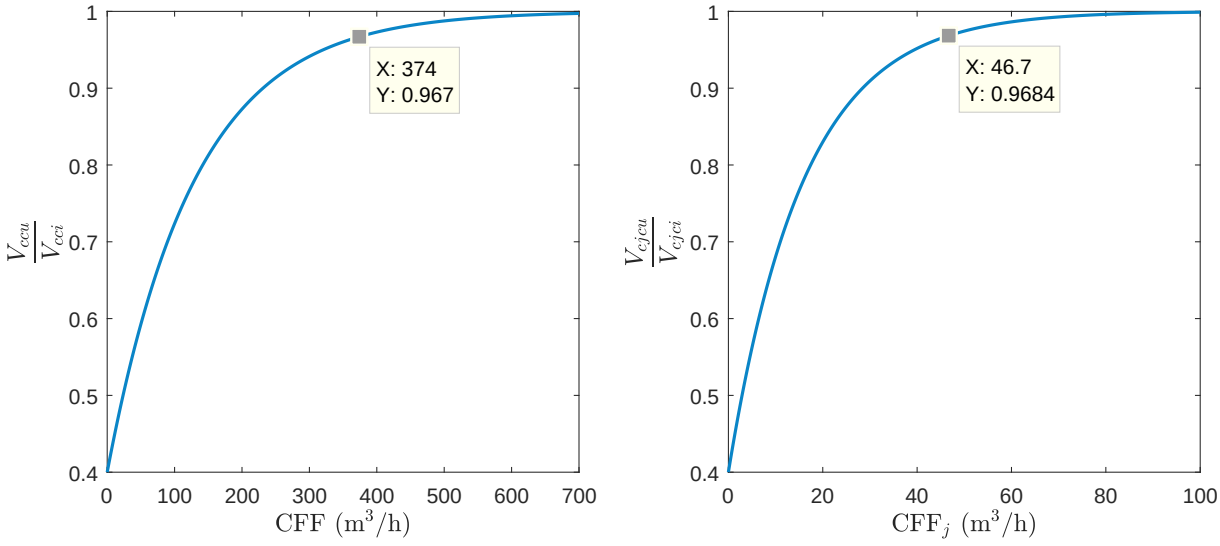

Figure 3.2. Course split for the original hydrocyclone (left) and the smaller new hydrocyclones (right).

Table 3.4. Individual hydrocyclone parameters in the cluster

Parm	Value	Description
α_{su}	0.915	Parameter related to fraction solids in underflow
C_1	0.6	Constant
C_2	0.7	Constant
C_3	4.0	Constant
C_4	4.0	Constant
ε_c	15.867	Parameter related to coarse split [m^3/h]

With the new value of ε_c, the hybrid model containing the switching dynamics is fully defined and at the correct steady-state when simulated. This shows that the hydrocyclone parameters were refitted correctly and that the circuit of [1] was correctly adapted to have a hydrocyclone cluster with eight nominal hydrocyclones. The nomenclature is given in Table 3.4.

Steady-state operation was validated by solving the complete hybrid model using a 4th order Runge Kuta function with all inputs and initial states at their normal values and observing that the derivatives of the states remained at zero. The nominal values were taken from [1]. The steady-state simulation is shown in Figure 3.3 and from the results it can be seen that there is no change in any output variable while all plant inputs are constant.

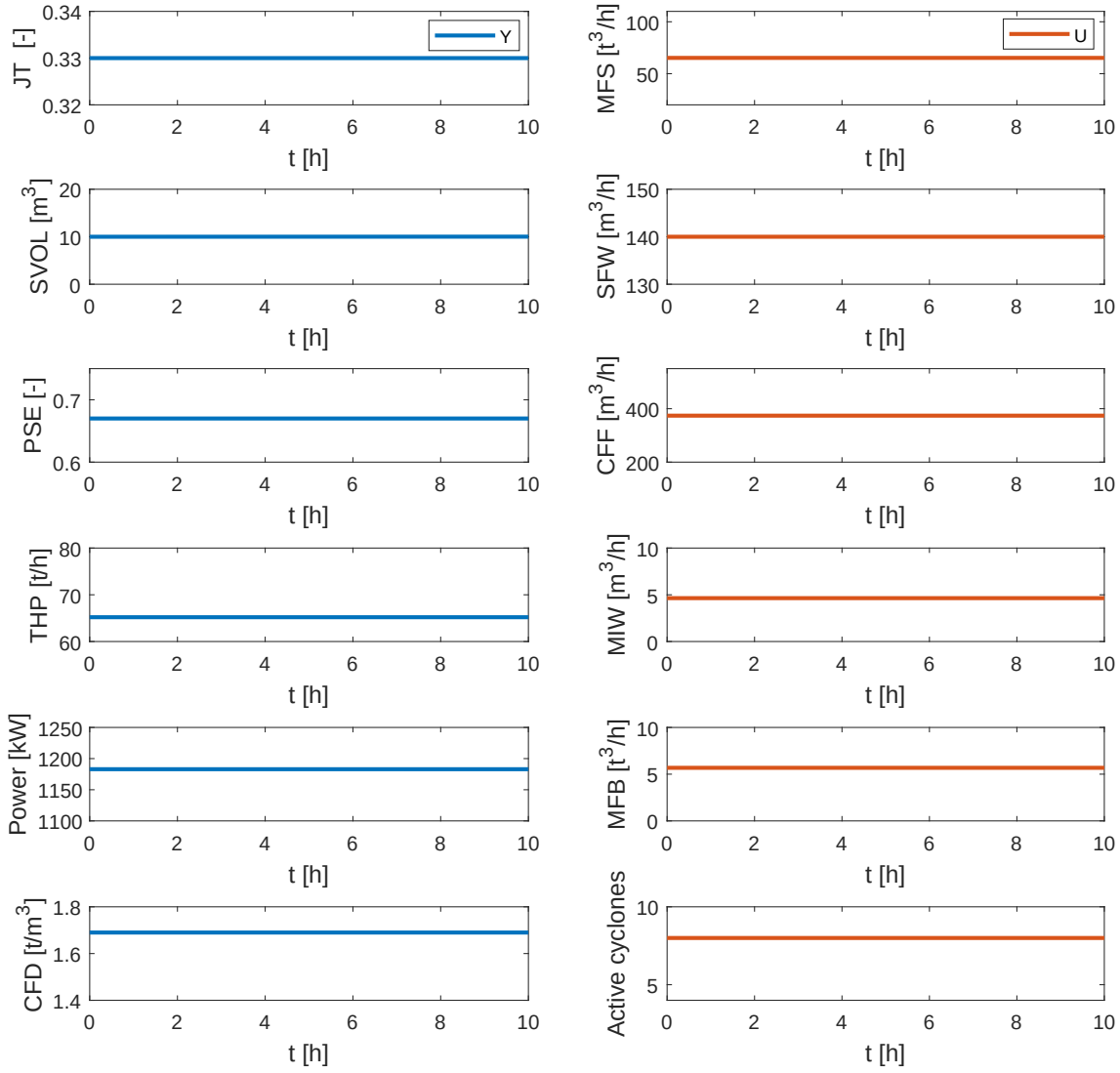

Figure 3.3. Simulation outputs (Y) on the left as a result of the constant process inputs on the right (U) to validate steady-state operation.

3.6 CONCLUSION

In this chapter a complete hybrid non-linear model for a grinding mill circuit with a cluster of hydrocyclones was presented. The model is sufficient for simulation and control purposes.

The model is presented in a modular way and the method to expand the single hydrocyclone to a cluster of hydrocyclones was prepared in enough detail so that the process can be repeated to include

additional discrete input variables. The chapter therefore not only details the grinding mill model, but creates a framework for expanding a grinding mill model to a hybrid model.

The number of hydrocyclones chosen in this chapter is based on previous studies where the need for hydrocyclone clusters arose. Furthermore, the number of hydrocyclones makes the discrete input variables (number of active hydrocyclones) a viable CV, as one switching event will not be drastic enough to force uncontrolled instabilities in the process.

The model is used for the NMPC and HNMPC controller formulation in Chapter 4, and for the simulation study in Chapter 5. Furthermore, the model as presented here was published as part of an NMPC study paper where the hydrocyclones were manually switched [12].

CHAPTER 4 CONTROLLER DESIGN

4.1 CHAPTER OVERVIEW

This chapter contains the core of this study, as it details how discrete inputs (in the form of switching hydrocyclones in a cluster) can be included directly in an APC controller. This chapter details the formulation of three different control schemes:

1. an NMPC controller,
2. an HNMPC controller, and
3. an HNMPC controller with a throughput maximisation objective.

The NMPC controller will act as a base case to compare the HNMPC controller results to. As discussed in [7], one of the control objectives is to maximise throughput while maintaining *PSE*. With the additional MV (in the form of a number of active hydrocyclones) it is hypothesised that it can be used as an optimisation variable when all the regulatory CVs are at their respective setpoints. The HNMPC was expanded (as a third controller) by adding a linear optimisation objective to the controller to maximise throughput.

The three controllers designed in this chapter can address the following research outcomes:

- In a situation where severe process disturbances are introduced into the grinding mill circuit and the downstream *PSE* requirement is increased, the simulation will show whether HNMPC is a better regulatory controller than NMPC, given the additional discrete input variables.

- In the situation where the plant is at a stable operating point, the HNMPC controller with a linear optimisation objective will show whether the switching of hydrocyclones can be used as a functional MV to improve the economic performance of the plant.

All three controllers use the model described in Chapter 3. In the case of the NMPC the number of active hydrocyclones is fixed to the nominal value of eight, which will ensure that there are no discrete dynamics or discontinuities that can hinder the performance of the controller.

A simulation and comparison of the controllers in this chapter are given in Chapter 5.

4.2 MUTUAL CONTROLLER DESIGN ELEMENTS

The three controllers follow the same execution process. NMPC utilises a plant model (for all three controllers it will be the model in Chapter 3, with the exception that $N_{ActiveCyclones}$ is clamped to 8 for the NMPC) to predict the future trajectory of the plant outputs (CVs) based on current inputs, outputs and states. The MPC controller calculates the MVs (also referred to as control moves) over a control horizon that will drive the plant outputs to their desired values over a prediction horizon by minimising an objective function. The objective function is minimised using an appropriate solver. The objective function is set up such that optimal steady-state operation can be achieved (through the most optimal control moves). The controller predicts an array of control moves, N_c, to drive the plant to the optimal state over the prediction horizon (N_p) at each iteration. At each iteration only the first control move (the first set of manipulated variables in N_c) is implemented, and the process is repeated. This is referred to as a receding horizon approach, which can be formulated from [64] as:

$$\min_{u_k,\cdots,u_{k+N_c-1}} J(u_k,\cdots,u_{k+N_c-1},x_k) \tag{4.1a}$$

$$\texttt{s.t.}\, x_{k+1} = f(x_k,u_k) \tag{4.1b}$$

$$y_k = h(x_k) \tag{4.1c}$$

$$u_l \leq u_k \leq u_u \tag{4.1d}$$

$$y_l \leq y_k \leq y_u \tag{4.1e}$$

where u_l and u_u represent the lower and upper limits (hard constraints) of the MVs respectively, and y_l and y_u represent the lower and upper limits of the CVs respectively. f and h are the discretised models

of (3.15). The initial states are given in Table 4.1 and the initial conditions and operating limits for the CVs and MVs are given in Table 4.2.

Table 4.1. Initial states used by NMPC and HNMPC

State	Initial Value	Unit
X_{mw}	4.6295	[m^3]
X_{ms}	4.6533	[m^3]
X_{mf}	0.9611	[m^3]
X_{mr}	1.9946	[m^3]
X_{mb}	8.2321	[m^3]
X_{sw}	6.8636	[m^3]
X_{ss}	3.1364	[m^3]
X_{sf}	0.6478	[m^3]

Table 4.2. Initial conditions and operating limits used by NMPC and HNMPC

Variable	Initial Value	Min	Max	Unit
Manipulated Variables				
MFS	65	0	200	[t/h]
MIW	4.65	0	100	[m^3/h]
SFW	140.47	0	300	[m^3/h]
CFF	374	200	450	[m^3/h]
$N_{ActiveCyclones}$	8	6	9	[-]
Controlled Variables				
J_T	0.33	0.2	0.4	[-]
$SVOL$	10	2.5	38	[m^3]
PSE	0.67	0.5	0.8	[-]

The three regulatory CVs are J_T, PSE, and $SVOL$. For this study J_T and PSE are controlled at setpoint, while $SVOL$ is controlled in a range between low and high soft limits. A soft limit is used for a PV controlled in a range which is still well within the hard constraints of the variable. Hard constraints are the absolute MV limits which should be exceeded and are typically as a result of some physical

limitation, exceeding the hard limits could cause process instabilities or lead to process upsets (such as a tank overflowing, or a plant shut down). The optimisation CV is THP.

For the base case NMPC controller where the number of active cyclones remain constant, the available MVs and CVs are:

$$u = [MFS, SFW, CFF]^T \tag{4.2a}$$

$$y = [J_T, SVOL, PSE]^T. \tag{4.2b}$$

For the HNMPC controller to be able to switch the hydrocyclones, the available MVs and CVs are:

$$u = [MFS, SFW, CFF, N_{ActiveCyclones}]^T \tag{4.3a}$$

$$y = [J_T, SVOL, PSE]^T. \tag{4.3b}$$

For the HNMPC to be able to switch the hydrocyclones with an optimisation objective to maximise throughput, the available MVs and CVs are:

$$u = [MFS, SFW, CFF, N_{ActiveCyclones}]^T \tag{4.4a}$$

$$y = [J_T, SVOL, PSE, THP]^T. \tag{4.4b}$$

In the above MV vectors MIW and MFB are not included as direct manipulated variables. MIW is kept at a constant ratio of the MFS. The ratio is determined at the initial steady-state as $\gamma_{MIW} = \frac{MIW_0}{MFS_0}$ and thereafter when using the model MIW is taken as $MIW = \gamma_{MIW} \times MFS$. In a SAG mill steels balls are commonly added at set time instances, and as balls are consumed in the mill over time they are replaced. In this study a continuous feed of steel balls is assumed. The feed rate of steel balls is set to a ratio of the mill filling. The ratio is defined by the initial steady-state as $\gamma_{MFB} = \frac{MFB_0}{J_{T0}}$ and throughout the simulation MFB is calculated as $MFB = \gamma_{MFB} \times J_T$.

With the controller execution methodology and the different MVs and CVs for each controller, the control elements that will remain the same for all the controllers are:

- The objective function will be identical for all three controllers. In the case of the NMPC and HNMPC where the optimisation objective is excluded, the linear optimisation weight will be zero.
- The weighting matrices will be identical. Although the HNMPC has an additional CV, the CV will not have a rate of change (ROC) penalty as the continuous input variables have. This is due to the fact that the penalty is inherently contained in the continuous CVs. One switching event results in immediate large changes in SFW and CFF. Therefore, a switching event will induce penalties in the objective function in the continuous variables. The identical weighting matrices also ensure that any differences in controller performance are not due to tuning, but merely result from the inclusion of hydrocyclone switching in the controller.
- To further ensure conformity between the controllers, N_p and N_c are also kept constant for all three controllers.

4.2.1 Objective function

The performance function, J, penalises large changes in MV moves, as well as any deviations from setpoint for the CVs or CV deviations beyond the soft limits. The controller objective function is adapted from [35] and is given as,

$$J(\cdot) = \sum_{n=0}^{N_p-1} \left[\left(y^r_{k+n|k} - \hat{y}_{k+n|k} \right)^T Q_r \left(y^r_{k+n|k} - \hat{y}_{k+n|k} \right) + S_{k+n|k} Q_s S_{k+n|k} + Q_l \hat{y}_{k+n|k} \right] + \sum_{n=0}^{N_c-1} \Delta u_{k+i|k}{}^T R \Delta u_{k+i|k} \tag{4.5}$$

where y^r is the CV setpoint, $\hat{y}$ is the predicted output, matrices Q_r, Q_s, Q_l and R are the weighting matrices for setpoint tracking, slack variables, linear optimisation objectives and control action movement respectively; and N_c and N_p are the control and prediction horizons respectively. The slack variable S is defined as,

$$S = \begin{cases} \hat{y} - y_{sh} & ; \hat{y} > y_{sh} \\ \hat{y} - y_{sl} & ; \hat{y} < y_{sl} \\ 0 & ; y_{sl} \leq \hat{y} \leq y_{sh}, \end{cases} \tag{4.6}$$

where y_{sh} and y_{sl} are the soft high and low limits respectively. If a soft limit is violated, the controller will control the violation in the same way as a setpoint deviation and will not regard it as an infeasible solution (which is the case when a hard constraint is reached). The quadratic function for setpoint

tracking will also ensure that if a specific CV cannot be maintained, given a disturbance or unachievable setpoint, the error will be distributed between the CVs based on the weighting matrices. If a linear objective function has been used for setpoint tracking the controller won't aim to maintain the setpoints, but rather ensure that the CVs are much higher than the setpoints in an attempt drive the setpoint deviation error to negative infinity to minimise the objective function. [35].

This study does not investigate the inclusion of a state estimator in the control loop and full-state feedback with normally distributed state noise is rather considered for feedback. Full-state feedback is a significant assumption, as the measurements available in industrial grinding mill circuits are limited [7]. Although various state estimators have been investigated for grinding mills [42, 50, 52, 51], it remains a challenge to estimate mill hold-ups [15, 47]. In the aforementioned state estimators the average predicted state error was less than 2%, which gives sufficient confidence that state noise with a 2% normal distribution can be used to test the controller performance with state errors.

4.2.2 Controller weights

For the controller set-up, the strongest emphasis is placed on maintaining PSE and J_T at setpoint. PSE is important for successful concentration of valuable metals in the downstream processes and is a key performance indicator that should be tightly controlled. J_T should also be controlled to ensure the integrity of the SAG mill and reduce downtime due to maintenance.

The Q_r and Q_s weighting matrices were formulated by ensuring that when PSE or J_T deviates from the setpoint by 1%, the effect on the objective function will be the same as when $SVOL$ deviates 5% from its soft limits. This ensures that the controller will be equally aggressive in bringing PSE and J_T back to setpoint, but less aggressive with $SVOL$.

Mathematically this can be represented as,

$$Q_{r1}\left(1\%JT_{SP}\right)^2 = Q_{r2}\left(1\%PSE_{SP}\right)^2 = Q_s\left(5\%SVOL_{sl}\right)^2. \tag{4.7}$$

The setpoints for J_T and PSE are taken as the initial steady-state conditions in Table 4.2. The soft limits for $SVOL$ are chosen within the hard constraints in Table 4.2. The lower soft limit ($SVOL_{sl}$) is chosen as 10 m^3 (which is also the initial steady-state value of the model) and the upper soft limit

($SVOL_{su}$) is chosen as 35 m^3. These chosen values allow a big enough safety margin between the soft high and low, and the absolute high and low limits for the sump.

Similarly, the R weighting matrix for the input variables can be calculated by choosing that a 1% change in half the ranges of CFF, MFS and SFW will contribute the same to the cost function,

$$R_1\left(\frac{1\%MFS_{range}}{2}\right)^2 = R_2\left(\frac{1\%SFW_{range}}{2}\right)^2 = R_3\left(\frac{1\%CFF_{range}}{2}\right)^2. \tag{4.8}$$

The R matrix was scaled to produce 1% of the Q matrix contribution, or mathematically,

$$R_1\left(\frac{1\%MFS_{range}}{2}\right)^2 = 0.01Q_{r1}\left(1\%JT_{SP}\right)^2. \tag{4.9}$$

By choosing $Q_s = 10$, the weighting matrices are calculated from (4.7) by using the initial simulation setpoints from Table 4.2 as,

$$Q_r = 10^3\begin{bmatrix} 230 & 0 \\ 0 & 55.7 \end{bmatrix}. \tag{4.10}$$

By using the result from (4.10) and the ranges in Table 4.2 with the relation in (4.9), the R weighting matrix can be calculated as,

$$R = \begin{bmatrix} 0.025 & 0 & 0 \\ 0 & 0.0111 & 0 \\ 0 & 0 & 0.0082 \end{bmatrix}. \tag{4.11}$$

Figure 4.1 visually shows the effect of PSE, J_T, and $SVOL$ deviations on the objective function. A 10% J_T error (the setpoint is 0.33 and therefore an error of 0.033) will add 250 to the objective function in (4.5). Similarly, a 10% PSE error (i.e. an error of 0.067 from the setpoint of 0.67) will add 250 and a 50% error in $SVOL$ from either of the soft limits will also add 250. The $SVOL$ error will be zero for the allowed buffer range, and hence an error will only occur once the soft limits are exceeded. This effect is illustrated in the bottom left graph of Figure 4.1. In the bottom right of Figure 4.1 it can be

seen that the *SVOL* error has a continuous quadratic influence on the objective function, however the discontinuity is contained in calculating the error from the PV (as shown in the bottom left graph of Figure 4.1). The graphs in Figure 4.1 therefore show that the design criteria to rank the importance of the CVs are achieved with Q_R and Q_s.

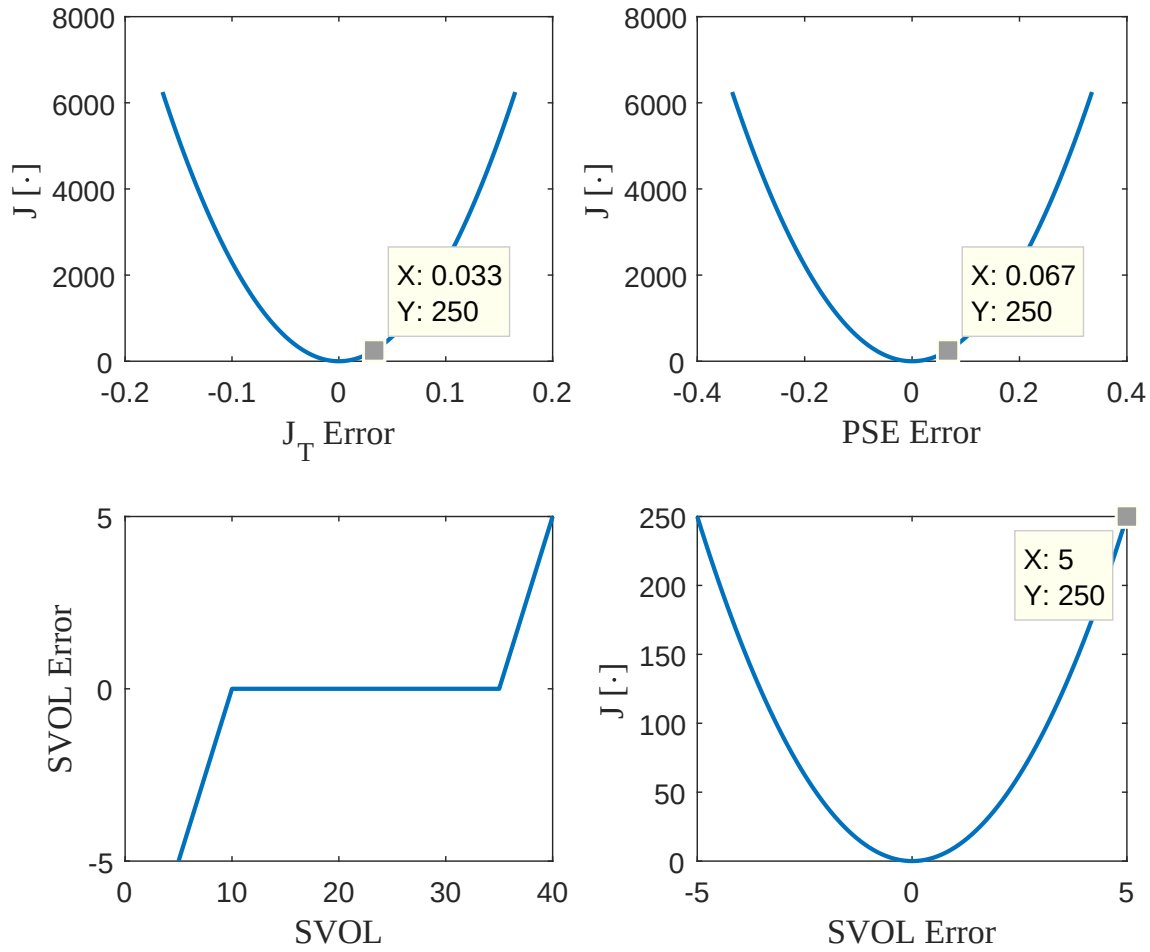

Figure 4.1. Effect of J_T Error (top left), *PSE* Error (top right), and *SVOL* Error (bottom right) on $J(\cdot)$. Bottom left shows the *SVOL* Error due to the value of *SVOL*

For the NMPC and HNMPC without the linear optimisation objective, Q_l is set to zero. In the case where the LP objective is included, Q_l needs to maximise *THP* and should be chosen as a negative number. The optimisation weight will improve the dynamic performance of the controller as long as the steady-state and dynamic optimisation objectives do not clash [35]. Therefore the weight Q_l was chosen as $Q_l = -2$. This ensures that if there is room for dynamic optimisation while the circuit is stable, the controller will consider it, but the steady-state objective weights still have a larger effect on $J(\cdot)$, should a setpoint deviation occur.

4.2.3 Prediction and control horizons

The prediction horizon, N_p, should generally be chosen such that the longest settling time for all of the outputs are observed [58]. Using the model in Chapter 3 and stepping MFS up by 1% for 50 min, then SFW down by 1% for 50 min, and then finally CFF up by 1% for 50 min, yields the simulation results shown in Figure 4.2. It can be seen that PSE and THP settle with the longest settling times of about 5 min. J_T and $SVOL$ are integrators and do not have settling times. The step test results show that the integrators have a comparable ROC with the responses of PSE and THP. Therefore, considering the step test data in Figure 4.2, it was decided that with a sampling time of T_s = 10 s, the prediction horizon is N_p = 36 (6 minutes). The control horizon was chosen as half of the prediction horizon N_c = 18 (3 minutes).

4.3 NMPC IMPLEMENTATION

The NMPC controller is implemented by firstly clamping $N_{ActiveCyclones}$ to 8 to ensure the model is a non-linear model and not a hybrid model. The controller is formulated such that current plant inputs, outputs and states are available (regardless of whether the states are available from full-state feedback or a state estimator). The objective function in (4.5) is then minimised using an array of $u = [MFS, SFW, CFF]^T$ (of length N_C) with predictions made using a 4th order Runge-Kutta function solving the model in Chapter 3. Minimisation is done using the *fmincon* function with the sequential quadratic programming (*sqp*) algorithm in MATLAB[1]. Once the optimal sequence of control moves has been found, only the first move is implemented. The controller is seeded with the past best fit sequence of control moves to reduce the computational burden. The algorithm can solve complex non-linear quadratic problems with hard constraints contained in a constraint function. The constraint function is the inequality constraints of all the MVs given in Table 4.2 and can be represented as:

$$E(u(k)) \geq 0 \tag{4.12a}$$

$$E = min\left[\overline{C} - u_k, u_k - \underline{C}\right] \tag{4.12b}$$

$$\overline{C} = [MFS_{max}, SFW_{max}, CFF_{max}] = [200, 300, 450] \tag{4.12c}$$

$$\underline{C} = [MFS_{min}, SFW_{min}, CFF_{min}] = [0, 0, 200]. \tag{4.12d}$$

[1]MATLAB is a registered trademark of The MathWorks Inc.

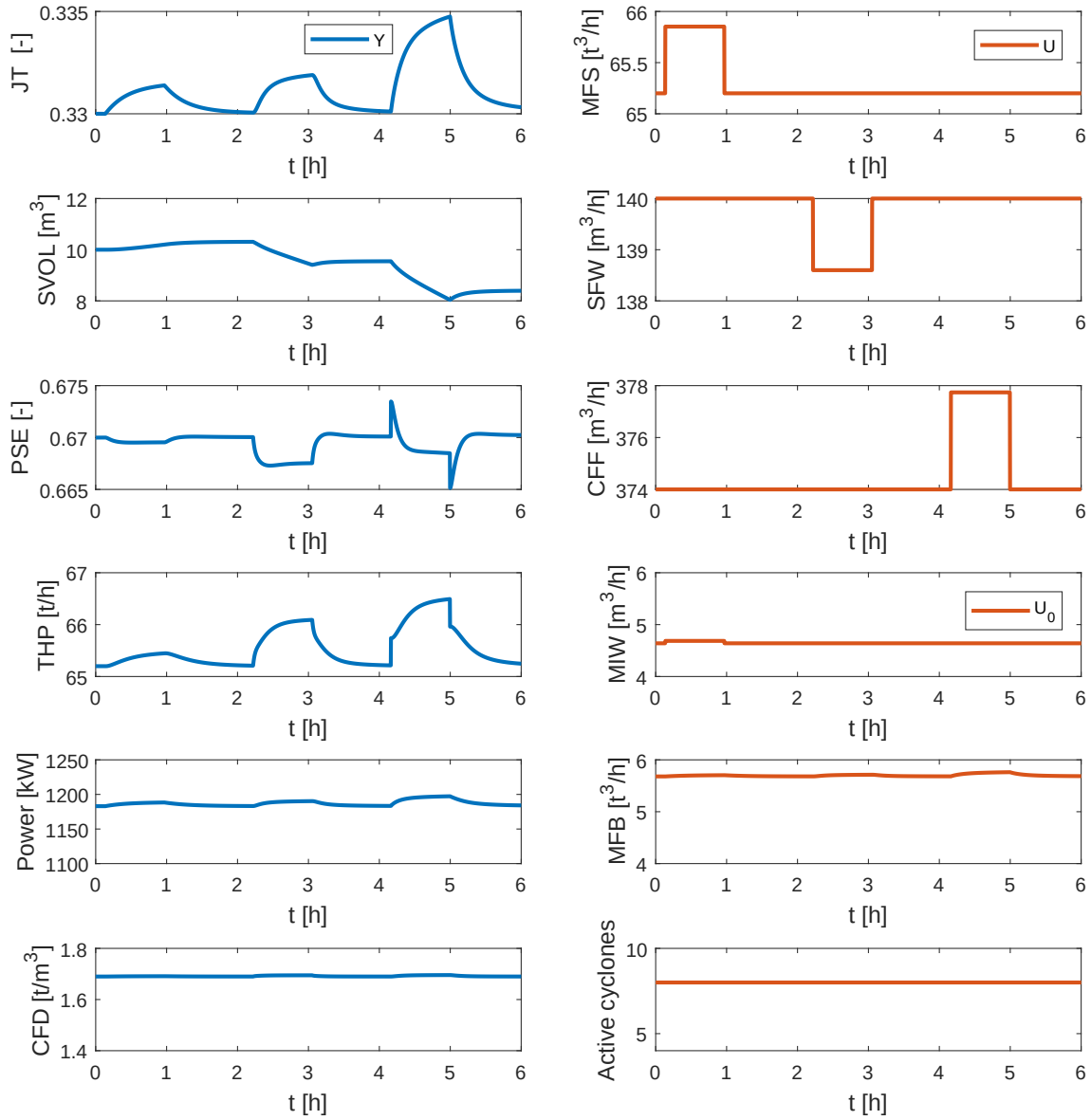

Figure 4.2. Open loop step test data to identify longest settling times in the grinding mill circuit. Simulation outputs are shown on the left and plant inputs on the right.

The *fmincon* settings were kept at their default values, except for the algorithm which was changed to *sqp*, the maximum number if iterations and the function tolerance. The maximum number of iterations were chosen as 10 to ensure that in a case where steady-state could not be achieved over the prediction horizon, the controller did not exceed the maximum allowed controller execution time. The function tolerance was chosen as 0.1 since it is a good indication of convergence given the objective function. The *fmincon* settings used for the NMPC are as follows:

- Algorithm = 'sqp'.
- MaxIter = 10.
- TolFun = 0.1.

4.4 HNMPC IMPLEMENTATION

The HNMPC controller is implemented similarly to the NMPC. The controller is formulated such that current plant inputs, outputs and states are available (regardless of whether the states are available from full-state feedback or a state estimator). The objective function in (4.5) is then minimised using $u = [MFS, SFW, CFF, N_{ActiveCyclones}]^T$ with predictions made using a 4th order Runge-Kutta function solving the model in Chapter 3.

Since hybrid dynamics are introduced in the circuit the solver should be able to minimise the objective function using continuous and integer control moves. As discussed in Section 2.6.2.1, the GA is an optimisation algorithm that has the ability to accommodate strong non-linearities, large variations in initial "guess" inputs, mixed integer dynamics (with various switching components) and convergence to a global minimum in the presence of many local minima [20, 62].

It is assumed that the hydrocyclone switching is done through solenoid valves at the input inlet of each individual hydrocyclone. The assumption is that the solenoid valves are fail-open to ensure that the CFF pump is protected from deadhead at all times. For this reason the controller output for the cluster should be an array of nine activation variables, where each activation variable is wired as a digital output to the corresponding solenoid. An example of the controller output when eight hydrocyclones are active is,

$$\rho(k) = [1,1,1,1,1,1,1,1,0]. \tag{4.13}$$

It should be noted that for a live implementation, the array in (4.13) will be implemented with reverse logic so that (considering 24 V solenoids):

$$1 = \text{Hydrocyclone ON} = 0\text{VDC to the solenoid} \tag{4.14a}$$

$$0 = \text{Hydrocyclone OFF} = 24\text{VDC}. \tag{4.14b}$$

If the HNMPC controller needs to solve the vector $\rho(k)$ in (4.13) it has to solve nine integer variables per execution. The computational burden per execution can be reduced by only solving one integer MV

($N_{ActiveCyclones}$). This approach reduces the computation time of the controller and is valid as long as identical hydrocyclones are used. In the case where the discrete variable models differ, the controller could aim to switch on a specific element, and in that case the entire array should be solved and not just the summation of activation variables. Similar to a running industrial plant, the model in Chapter 3 uses the complete vector of activation variables, and therefore the controller solves $N_{ActiveCyclones}$ but in the model it is first converted to the correct vector.

In addition, the switching of hydrocyclones has a large dynamic influence on the plant, and in order to avoid sporadic switching leading to plant instability, hydrocyclones can only be switched once every two prediction horizons. Continuous control moves are therefore made at every interval over the control horizon, while hydrocyclone switching can only be done once (on condition a switching event did not occur within the previous 12 minutes).

As discussed in Chapter 3, the cluster contains nine hydrocyclones and a minimum of six should be active. The CFF constraint in Table 4.2 is the total feed to the hydrocyclone cluster at nominal conditions (eight active hydrocyclones). Therefore, when the hydrocyclones in the cluster are switched, the constraint for CFF changes. The discrete dynamics will therefore also have an effect on the inequality constraint function and therefore (4.12) for the HNMPC becomes

$$E_2(u(k)) \geq 0 \tag{4.15a}$$

$$E_2 = min\left[\overline{C} - u_k, u_k - \underline{C}\right] \tag{4.15b}$$

$$\overline{C} = [MFS_{max}, SFW_{max}, CFF_{max}, N_{ActiveCyclones-max}] = [200, 300, (4.15e), 9] \tag{4.15c}$$

$$\underline{C} = [MFS_{min}, SFW_{min}, CFF_{min}, N_{ActiveCyclones-min}] = [0, 0, (4.15f), 10] \tag{4.15d}$$

$$CFF_{max} = 450\frac{N_{ActiveCyclones}}{8} \tag{4.15e}$$

$$CFF_{min} = 200\frac{N_{ActiveCyclones}}{8}. \tag{4.15f}$$

The number of active cyclones does not influence the constraints for the feed to the mill, or the flow rate of water to the sump. Similar to *fmincon*, the MV constraints are added directly to the *ga* function, ensuring a feasible solution in all operating conditions.

The MATLAB *ga* function was used to implement the GA to form the HNMPC solution. The controller can only solve one input array, and therefore one temporary array (containing all the control moves

over the control horizon) is added to the *ga* function to be solved. The first 18 variables in the array are the movement of u_1 over the control horizon, the next 18 are u_2, the 18 thereafter are u_3, and the last variable is $N_{ActiveCyclones}$. $N_{ActiveCyclones}$ is only added once, since it is not solved for each iteration in N_c, as only one switching event is allowed (since a hydrocyclone can only be switched once every 12 minutes). As a result the number of elements to be solved is 55.

The settings for the *ga* function that follow were chosen based on the dynamics of the system, computational load and robustness of the controller performance:

- The fitness function is the non-linear quadratic objective function in (4.5).
- 'FitnessLimit' = 0.1; if the objective function attains the fitness limit, the GA halts.
- 'TolFun' = 0.1; if the relative change in the objective function is less that the function tolerance the GA halts.
- 'InitialPopulation' = the previous optimal solution (all 55 variables); in seeding the solver the computational burden is reduced in finding the optimal solution, but owing to the stochastic nature of the algorithm the seed will not cause the solver to get stuck at a local optimum.
- 'PopulationSize'= 50; the population size is the number of possible best fit individuals.
- 'Generations' = 35; the maximum number of generations limits the function iterations if the function tolerance cannot be obtained over N_p.
- 'nvars' = 55; nvars is the number of individuals to be solved, i.e. the three continuous MVs over N_c and the one integer MV.
- 'nonlcon' = (4.15); the inequality constraints for the CVs.
- The rest of the settings were evaluated but kept at the default values, considering the nature of the control problem:
  - CrossoverFcn = intermediate.
  - CrossoverFraction = 0.8.
  - EliteCount = ceil(0.05×PopulationSize).
  - MaxTime = Infinity.

4.5 CONTROLLER SETTINGS SUMMARY

A summary of the controller settings is shown in Table 4.3.

Table 4.3. Controller settings for the NMPC, HNMPC, and HNMPC with throughput maximisation

Setting	**NMPC**	**HNMPC**	**HNMPC with THP maximise**
$J(\cdot)$	$\sum_{n=0}^{N_p-1}\left[\left(y^r_{k+n\|k}-\hat{y}_{k+n\|k}\right)^T Q_r\left(y^r_{k+n\|k}-\hat{y}_{k+n\|k}\right)+S_{k+n\|k}Q_sS_{k+n\|k}+Q_l\hat{y}_{k+n\|k}\right]+\sum_{n=0}^{N_c-1}\Delta u_{k+i\|k}{}^T R\Delta u_{k+i\|k}$		
T_s	10s	10s	10s
MVs	$[MFS, SFW, CFF]$	$[MFS, SFW, CFF, N_{ActiveCyclones}]$	$[MFS, SFW, CFF, N_{ActiveCyclones}]$
CVs	$[J_T, SVOL, PSE]$	$[J_T, SVOL, PSE]$	$[J_T, SVOL, PSE, THP]$
$\overline{u}$	$[200, 300, 450]$	$[200, 300, 450\frac{N_{ActiveCyclones}}{8}, 9]$	$[200, 300, 450\frac{N_{ActiveCyclones}}{8}, 9]$
$\underline{u}$	$[0, 0, 200]$	$[0, 0, 200\frac{N_{ActiveCyclones}}{8}, 6]$	$[0, 0, 200\frac{N_{ActiveCyclones}}{8}, 6]$
N_p	36 (6min)	36 (6min)	36 (6min)
N_c	18 (3min)	18 (3min)	18 (3min)
Q_r	$\text{diag}(10^3[230, 0, 55.7])$	$\text{diag}(10^3[230, 0, 55.7])$	$\text{diag}(10^3[230, 0, 55.7, 0])$
Q_s	$\text{diag}([0, 10, 0])$	$\text{diag}([0, 10, 0])$	$\text{diag}([0, 10, 0, 0])$
Q_l	[]	[]	$\text{diag}([0, 0, 0, -2])$
R	$\text{diag}([0.025, 0.0111, 0.0082])$	$\text{diag}([0.025, 0.0111, 0.0082, 0])$	$\text{diag}([0.025, 0.0111, 0.0082, 0])$
Solver	*fmincon* with *sqp*	Genetic Algorithm	Genetic Algorithm

4.6 CONCLUSION

In this chapter three different controllers were formulated:

- a base case NMPC controller to compare the HNMPC controller to,
- an HNMPC controller capable of switching hydrocyclones in a cluster, and
- an HNMPC controller with an optimisation objective to maximise THP.

The design and implementation of the NMPC as presented in this chapter are described in [12].

The HNMPC controller uses an evolutionary algorithm known as a GA. The GA has many advantages over other solvers, but can be computationally demanding. The HNMPC formulated in this chapter

addressed the computation requirements of the GA by applying certain programmatic techniques, and the required computational time was further reduced by critically evaluating the GA options (when using the *ga* toolbox in MATLAB) and carefully selecting them to weigh off controller execution time, solution quality and controller robustness. A simulation and comparison of the controllers are given in Chapter 5.

CHAPTER 5 SIMULATION RESULTS AND DISCUSSION

5.1 CHAPTER OVERVIEW

In this chapter the controllers in Chapter 4 are simulated and the results discussed. The controller performance is evaluated in terms of setpoint tracking and optimisation. Large plant disturbances and setpoint changes are made during simulation. The base case (NMPC) controller is compared to the HNMPC and a performance metric is used to quantify the benefit over the simulation duration.

5.2 SIMULATION SCENARIO

The aim of the simulation is to disturb the plant (initially at steady-state), and observe how the NMPC and HNMPC controllers react to the disturbance. The simulation conditions should provide a scenario where the following research questions can be answered:

- Does the HNMPC have better disturbance rejection over the NMPC because it can switch the hydrocyclones?
- In cases where the steady-state operating requirements (e.g. PSE setpoint changes as a result of downstream requirements) change to an unachievable value owing to the ore feed hardness and the circuit capabilities, will the HNMPC outperform NMPC by using the hydrocyclone cluster switching as an additional handle?
- In the case where steady-state operation is achieved, but there is the possibility to increase THP by increasing the cluster feed capacity, will the HNMPC with throughput maximisation switch hydrocyclones to maximise THP while maintaining all other setpoints?

The simulation study is partly formulated from the approach in [13] where ore can be fed to the mill from different stockpiles with various ore hardness. Since the ore does not undergo any pre-processing, any change in feed ore composition and hardness will have an immediate effect on the circuit performance. Therefore, the disturbances that will be added to the simulation are a change in ore hardness and feed size distribution that correlates to a scenario where a different stockpile is fed to the mill. Similar to viewing the benefits of having an HNMPC running over an NMPC when a plantwide control structure is implemented, the PSE setpoint will be changed more regularly throughout the simulation to simulate a condition where the downstream process changes the desired steady-state operating condition. By adding these constant disturbances and frequent setpoint changes, the two HNMPC controllers can be evaluated against the NMPC. Full-state feedback is assumed for the initial simulations. A final simulation is then run where 2% state noise is added to the HNMPC with THP maximisation to show the robustness of the controller even in the presence of measurement and state estimation errors. In all cases performance metrics are applied to quantify the controller benefits.

The simulation conditions can be summarised as,

- Simulation time of $T_f = 7$ h and a sampling rate of $T_s = 10$ s.
- The mill inlet water MIW is kept at a ratio of $\gamma_{MIW} = \frac{MIW_0}{MFS_0}$ to MFS and the feed rate of balls into the mill MFB is kept at a ratio of $\gamma_{MFB} = \frac{MFB_0}{J_{T0}}$ to J_T.
- Full-state feedback is assumed to compare the NMPC, HNMPC, and HNMPC with THP maximising, and thereafter 2% state noise is added to the HNMPC with THP maximising to show whether the advantages it has over the other two controllers hold even in the presence of state and measurement errors.
- At first the feed ore hardness is increased from the initial value and maintained, then it is greatly reduced (to below the initial feed ore hardness). The hardness of the ore is changed at
  - t = 12 min by increasing ϕ_f to 36.87 kWh/t and ϕ_r to 8.4 kWh/t from their nominal values of 29.5 kWh/t and 6.72 kWh/t respectively, and
  - t = 107 min by decreasing ϕ_f from 36.87 kwh/t to 19.2 kWh/t and ϕ_r from 8.4 kWh/t to 4.4 kWh/t.

- Another constant disturbance was added to test the controller's robustness in changing ore feed size distribution. These disturbances were added at
  - t = 230 min by increasing α_r to 0.765 from its nominal value of 0.465, and
  - t = 245 min by decreasing α_r from 0.765 to 0.365.
- J_T is kept constant at its nominal value of 0.33 throughout the simulation.
- $SVOL$ is allowed to drift between 10 m^3 and 35 m^3, but should be controlled back to the operating region if the soft limits are violated.
- PSE is changed to simulate a setpoint requirement from the downstream unit. The PSE setpoint was changed at
  - t = 30 min by increasing the setpoint from 0.67 (nominal value) to 0.73, and
  - t = 202 min by decreasing the setpoint from 0.73 to 0.64.

Figure 5.1 shows the disturbances added to the plant. The setpoint changes are shown as part of the controller results.

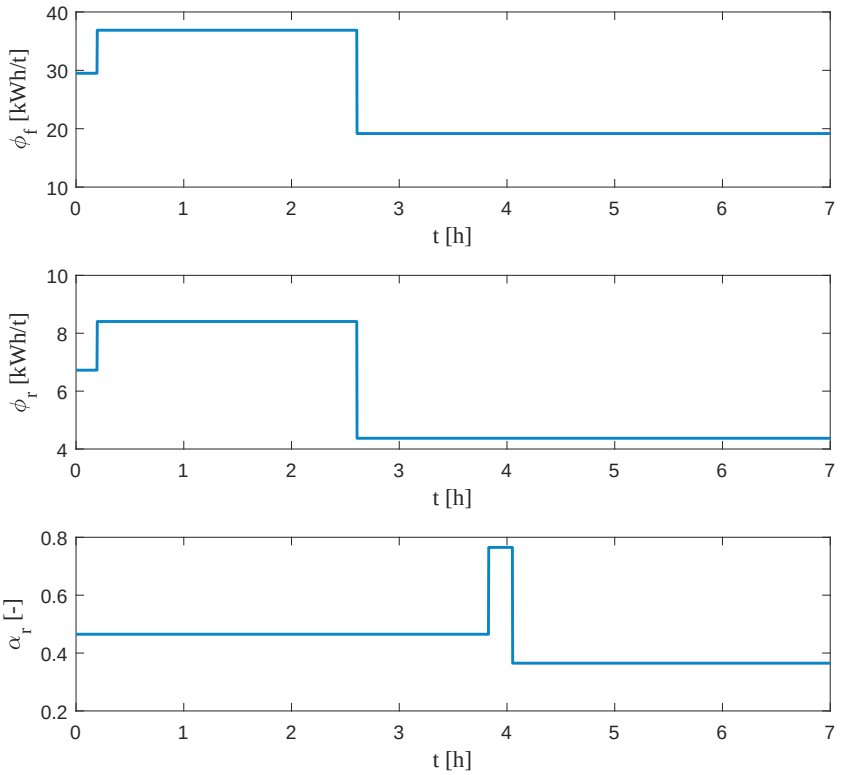

Figure 5.1. Disturbances added to the controller simulations. Top: Power needed per tonne of fines produced ϕ_f. Middle: Rock abrasion factor ϕ_r. Bottom: Fraction of rocks in the feed α_r.

5.3 CONTROLLER PERFORMANCE METRICS

The performance of the controllers needs to be quantified in order to evaluate and compare them. This section provides the metrics used to quantify the performance of the economic variables (PSE and THP) as well as the setpoint control of J_T. The deviation from setpoint for PSE and J_T is quantified by calculating the sum of all squared errors (similar to [5]),

$$PSE_{Performance} = \sum_{k=0}^{N_f} (PSE^r(k) - PSE(k))^2 \tag{5.1a}$$

$$J_{T\,performance} = \sum_{k=0}^{N_f} (J_T^r(k) - J_T(k))^2 . \tag{5.1b}$$

The average throughput for the duration of the simulation is calculated as,

$$THP_{Average} = \frac{1}{N_f} \sum_{k=0}^{N_f} THP(k). \tag{5.2}$$

A performance function for the mineral value is given in [25], which can be used when the circuit is at steady-state. The monetary value can be calculated as,

$$\psi[\$/h] = THP[t/h] \times \text{head grade}[g/t] \times \text{mineral price}[\$/g] \times \text{recovery}[\%] \tag{5.3}$$

where the head grade is defined in [5] as 3g/t, the recovery is a parabolic function of PSE as given in (2.1), and the mineral price for gold at the time of writing is \$40.03/g.

For the complete seven-hour simulation the performance metrics in (5.1) and (5.2) are used to evaluate the overall controller performance. In the case where the controller cannot maintain the setpoint, but settles to an achievable PSE, or if THP is maximised at steady-state, then (5.3) can be used to evaluate the monetary benefit of using HNMPC over NMPC.

5.4 RESULTS

5.4.1 NMPC results

Figure 5.2 shows the NMPC controller results for the simulation; the plant outputs are shown on the left, and the plant inputs (as a result of the NMPC control actions) are shown on the right.

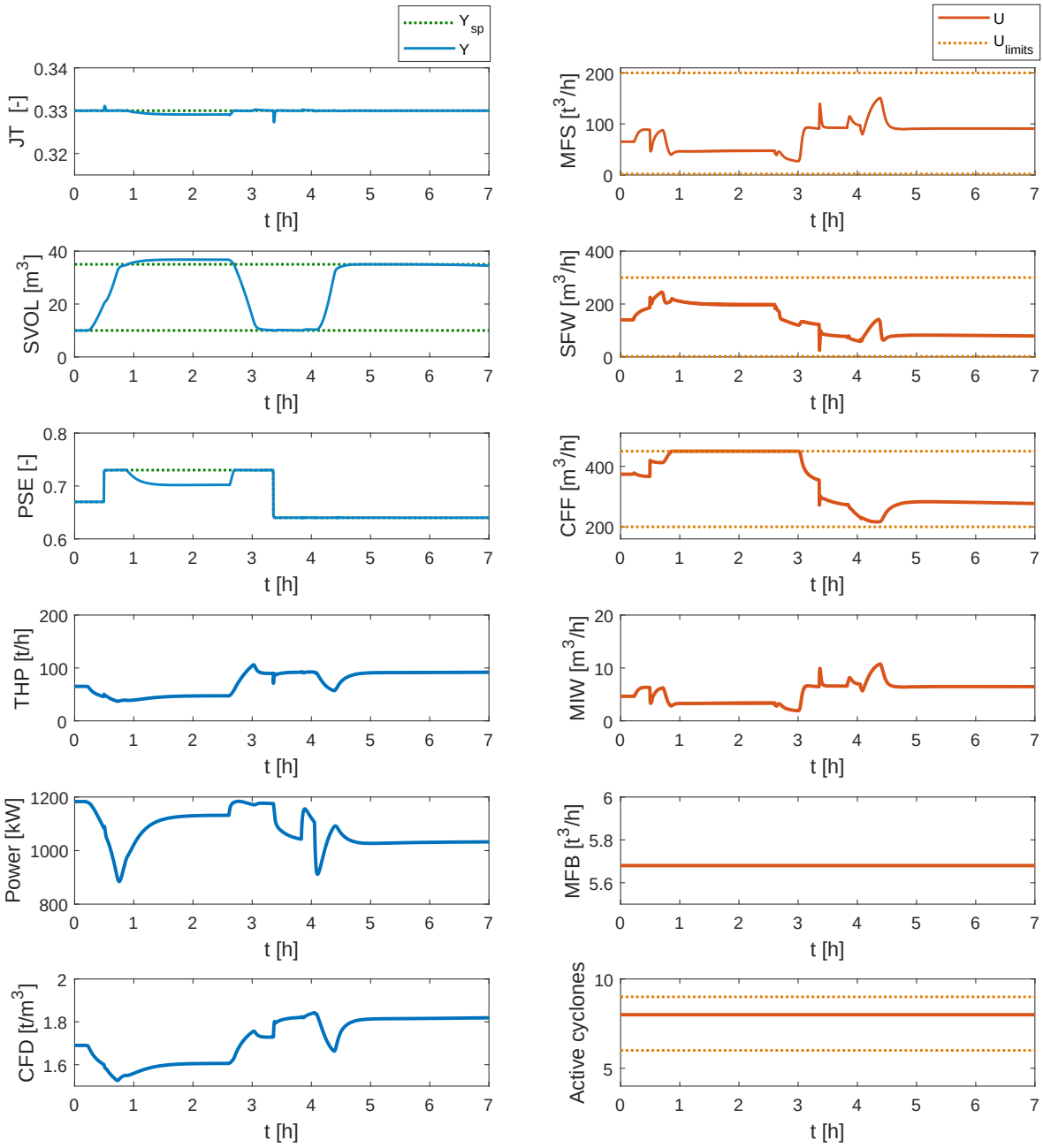

Figure 5.2. Simulation results for the NMPC controller.

Between t = 12 min and t = 30 min, the controller compensates for the initial hardness increase by decreasing CFF and increasing SFW (and allowing $SVOL$ to drift within its soft limits) to maintain sufficient classification with the reduced amount of fines discharged from the mill. A decrease in CFF and increase in SFW result in J_T decreasing and the controller increases MFS to maintain J_T. The controller maintains all setpoints and a slight reduction in THP is observed.

At t = 30 min, with the increase in the PSE setpoint, the CFF is increased to meet the PSE requirement. The PSE setpoint is maintained by controlling the CFD using SFW and CFF; however, $SVOL$ quickly reaches its upper soft limit and the controller increases CFF and decreases SFW to bring $SVOL$ back into limits. The desired PSE setpoint is unachievable and the controller settles to a steady-state condition where J_T also deviates slightly from setpoint, and PSE reaches a steady-state value of 0.7 (0.03 less than the setpoint).

At t = 107 min, when the hardness of the feed ore is decreased, the residence time of the material in the mill is reduced and more fines are discharged from the mill. The PSE setpoint is quickly recovered and with the increase in fines, less water is required in the circuit and SFW is reduced. The controller keeps CFF fixed, and the PSE setpoint quickly recovers with the increase in the discharge rate of fines from the mill. With the increase in material meeting the quality specification, more particles are discharged from the classifier, the circulating load reduces and the level of the sump decreases. The controllers reduce SFW in order to control the sump level.

At t = 202 min, when the PSE setpoint dropped, the controller decreased CFF and the setpoint was quickly achieved and maintained.

The controller adequately controlled the increase (at t = 230 min) and decrease (at t = 245 min to the end of the simulation) in the feed size distribution and no deviations were observed for J_T, $SVOL$, or PSE. A decrease in THP was observed when α_r was increased. This decrease was expected, since an increase in α_r increases the hold-up of rocks in the mill, and to control J_T the controller needs to reduce MFS, which results in decreased throughput.

The controller performance metrics as indicated in (5.1) and (5.2) for the seven-hour simulation are:

$$PSE_{Performance} = 0.4303$$

$$J_{Tperformance} = 0.0004$$

$$THP_{Average} = 72.39 \text{ t/h}.$$

5.4.2 HNMPC results

Figure 5.3 shows the HNMPC controller results for the simulation; the plant outputs are shown on the left, and the plant inputs (as a result of the HNMPC control actions) are shown on the right.

The HNMPC responds similarly to the NMPC in compensating for the hardness decrease (between t = 107 min and t = 202 min), and feed ore size distribution fluctuation (between t = 230 min and t = 270 min).

However, between t = 12 min and t = 30 min, with the initial increase in feed ore hardness, instead of decreasing CFF it was increased, and SFW was slightly increased to reduce the CFD and maintain hydrocyclone separation even with the reduced fines from the mill discharge. With the increase in CFF and decrease in THP, the circulating load is increased and therefore the slurry rheology factor in the mill does not increase as much as with NMPC and the reduction in P_{Mill} is not as large, indicating a better operating condition. This advantage is purely based on the solver used, and not a result of the discrete dynamics.

At t = 30 min, when the PSE setpoint is increased, the HNMPC switches off a hydrocyclone. The feed to the individual hydrocyclones should be high (to maintain sufficient separation), but owing to the reduced fines discharged from the mill, to maintain the mass balance in the sump the circulating load should be reduced and CFF should be reduced. These control actions are conflicting, but by switching off a hydrocyclone, CFF can be reduced while the individual hydrocyclone pressure and feed rate remain high enough to achieve sufficient separation. This results in a dynamic response where the sump fills more slowly, since less SFW is required because of the reduced circulating load. With the reduced ROC of the sump level, PSE is maintained for longer than with the $NMPC$ and once the sump reaches its upper limit, the steady-state PSE is 0.71 (which is only 0.02 from the setpoint).

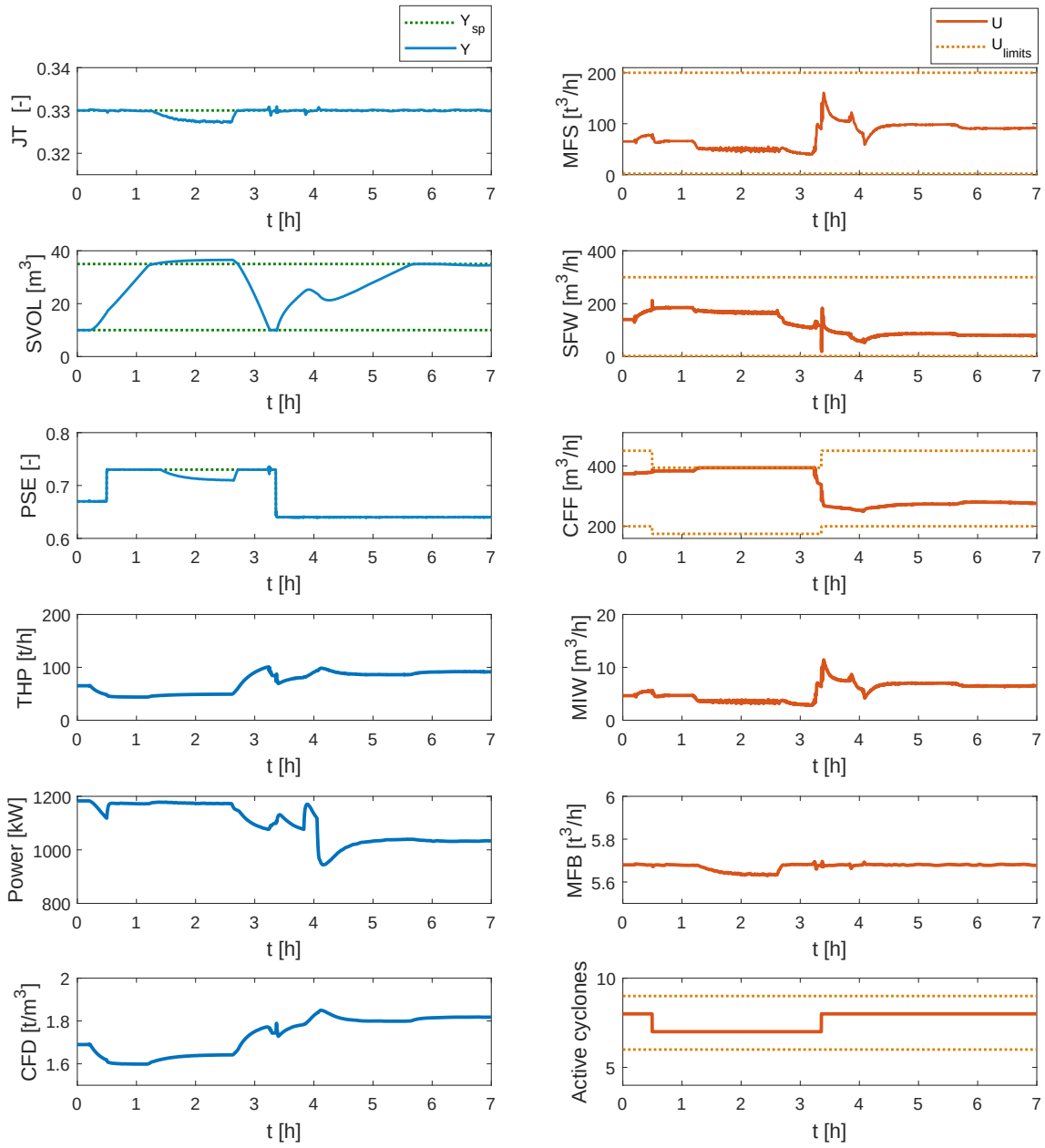

Figure 5.3. Simulation results for the HNMPC switching hydrocyclones.

However the J_T error is slightly larger than with the NMPC. Upon initial investigation it seemed that the controller could switch off an additional hydrocyclone to reduce the *PSE* error further. However, because of the switching rules (once a hydrocyclone is switched, another can only be switched in 12 min), by the time another hydrocyclone can be switched off, *PSE* is already decreasing, and all possible handles to maintain *PSE* are already at their limits. Therefore another hydrocyclone is not switched off. Directly including the discrete dynamics as part of the controller resulted in a much better dynamic response and a reduced error in *PSE*.

At t = 202 min once the *PSE* setpoint is reduced and with the softer feed ore, the HNMPC switches on an additional hydrocyclone to reach the setpoint. If a hydrocyclone was not switched (and only seven hydrocyclones were active), the controller could still reach the *PSE* setpoint. However, the CFF movement to achieve it will be much higher, and therefore switching on an additional hydrocyclone reduces the control movement required to achieve the steady-state requirement.

With the additional active hydrocyclone (just after t = 3 h) the circuit was again running with the nominal number of hydrocyclones and the HNMPC and NMPC performed similar control moves to reject the α_r disturbance.

The HNMPC controller performance metrics for the seven-hour simulation are:

$$PSE_{Performance} = 0.117$$

$$J_{Tperformance} = 0.0025$$

$$THP_{Average} = 72.86 \text{ t/h}.$$

The controller performance metrics indicate that the HNMPC significantly reduced the PSE_{Error} during the simulation by being able to use the hydrocyclone cluster. Overall it performed worse in controlling J_T but this was due to the controller being able to maintain *PSE* closer to its setpoint and therefore distribute more of the steady-state error to J_T as a result of the quadratic objective function. An increase in THP is also seen, which is a result of better dynamic responses by the HNMPC over the NMPC due to the additional control handle. When a grinding mill circuit is running at higher power, it can be assumed that THP is maximised [6]. According to the HNMPC and NMPC results P_{mill} is higher most of the time for the HNMPC.

5.4.3 HNMPC with throughput maximisation results

Figure 5.4 shows the HNMPC with THP maximisation controller results for the simulation; the plant outputs are shown on the left, and the plant inputs (as a result of the HNMPC with THP maximisation control actions) are shown on the right.

From the start of the simulation to t = 3.5 h, the controller performance is identical to the original HNMPC controller and the plant outputs are also identical.

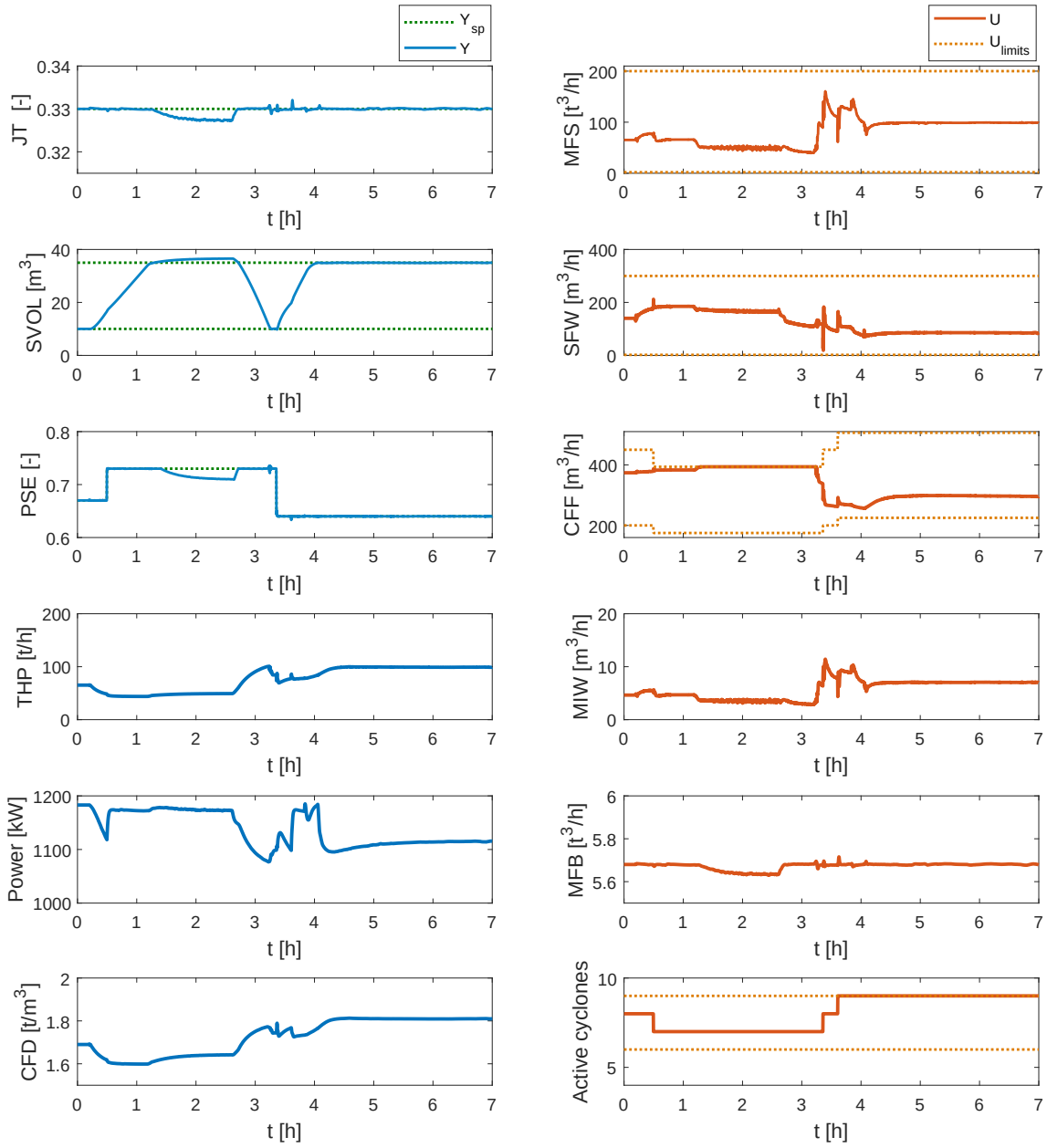

Figure 5.4. Simulation results for the HNMPC with THP maximisation.

However, at t = 202 min, after the PSE setpoint has been reduced and since the feed ore is softer than the nominal hardness, the controller switches on an additional hydrocyclone (the same as in Section 5.4.2), but 13 min later an additional hydrocyclone is switched in, taking the number of active hydrocyclones up from seven to nine. This control move is purely a result of the optimisation objective. With the softer ore and reduced quality specification, the mill can easily grind more material. However, with eight active hydrocyclones MFS cannot be increased in order to improve THP, since an increase in MFS will result in greater discharge of material from the mill, which increases the sump level. To

maintain CFD the feed rate of water to the sump cannot be reduced in order to maintain the sump level, and if CFF is increased to lower $SVOL$ the product quality will deviate from setpoint. Therefore in the simulation from 3.2 hours to the end (even with the α_r disturbance) THP can be maximised, but the hydrocyclone cluster is the bottleneck with eight active hydrocyclones. The HNMPC with THP maximisation identified this dynamic optimisation opportunity and by switching on an additional hydrocyclone, CFF is increased, thereby achieving the maximum possible MFS while maintaining the same circulating load. Therefore, all steady-state operating conditions are achieved, while throughput is maximised.

As shown in the early stages of the simulation (at t $\leq$ 107 min), if the controller can no longer maintain the high circulating loads and CFF needs to be reduced, then in order to maintain hydrocyclone efficiency the controller switches off some of the hydrocyclones to ensure that the regulatory control objectives are achieved.

The controller performance metrics for the seven-hour simulation are calculated as

$$PSE_{Performance} = 0.1173$$

$$J_{Tperformance} = 0.0025$$

$$THP_{Average} = 76.26 \text{ t/h}.$$

From the simulation results in this section and those in Section 5.4.2, the following conclusion can be drawn:

- It was necessary to simulate and test an HNMPC with and without an optimisation objective to ensure that the controllers were designed in such a way that the optimisation objective does not force the controller to become unstable in a case where the regulatory control objectives cannot be fully met.
- The results in this section showed that the objective function weights chosen allow for independent regulatory control and optimisation and that the optimisation objective will only warrant a control move if the setpoints can be maintained.

5.4.4 NMPC and HNMPC comparison of results

From the individual controller simulations, it was seen that the HNMPC controller performs much better when the optimisation objective is added to the objective function. In addition, the optimisation objective did not cause any instabilities when the plant was forced into an almost uncontrollable condition (this was seen by comparing the dynamic responses of the HNMPC and the HNMPC with THP maximisation). Therefore to evaluate the benefits of the HNMPC relative to the NMPC, only the HNMPC with THP maximisation has to be compared to the NMPC.

A summary of the overall controller performance metrics for the NMPC and HNMPC during the seven-hour dynamic simulation is given in Table 5.1. The HNMPC controller outperformed the NMPC, as the sum of squared PSE errors was reduced by 72.8% and THP was increased by 5.4%. The NMPC had a lower sum of squared errors for J_T, but maintaining J_T had no immediate economic effect and the error was still far from any limits.

Table 5.1. Controller performance comparison

Metric	HNMPC	NMPC
$PSE_{Performance}$	0.1173	0.4303
$J_{T\,performance}$	0.0025	0.0004
$THP_{Average}$	76.26 t/h	72.39 t/h

This section will therefore further compare the economic benefits of the controllers by considering not only the overall average or summed values, but also the specific steady-state operating conditions achieved during the simulation. This will highlight the economic advantages of using an HNMPC to include hydrocyclone switching dynamics over a conventional NMPC controller. The controller benefits are split into two sections:

- The first shows that in a case where the plant is almost uncontrollable, the HNMPC achieves better steady-state operation.
- The second compares the two controllers when there is a possible economic optimisation opportunity.

5.4.4.1 Setpoint tracking and disturbance rejection

Figure 5.5 shows a zoomed-in section (from 0.3 hours into the simulation to 3.4 hours) of the seven-hour simulation. The zoomed-in section focuses on the case where the desired *PSE* setpoint cannot be obtained, given the feed ore hardness and grinding circuit operating limitations.

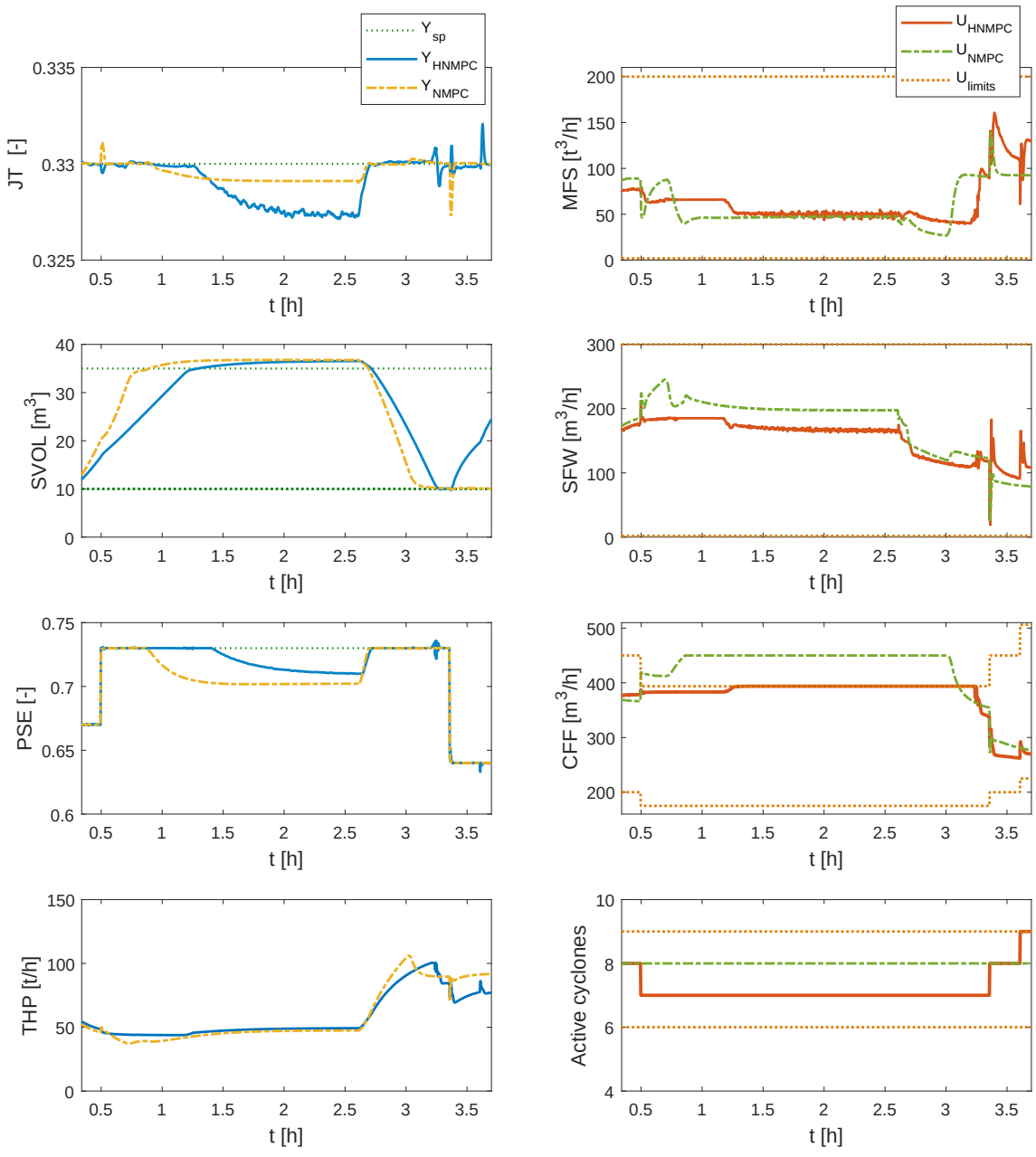

Figure 5.5. Comparison of the CVs responses for the HNMPC and NMPC with a large *PSE* setpoint and large feed ore hardness disturbance.

Both the NMPC and the HNMPC controllers reach a steady-state operating point where the error is distributed among the CVs. However, in the case of the HNMPC controller, the *PSE* error is much less (at the cost of a greater J_T error). Therefore, by using the monetary performance function in Section 5.3 for the two steady-state operating conditions, the monetary benefit obtained by including the mixed integer dynamics into the control problem (in the form of switching hydrocyclones) is calculated from (5.3) as

$$\psi_{NMPC} = 3906.60 \text{ \$/h}$$

$$\psi_{HNMPC} = 4066.18 \text{ \$/h}$$

$$\text{Economic benefit} = 159.58 \text{ \$/h}.$$

This equates to a per hour monetary improvement of 4% due to the better steady-state operating point.

5.4.4.2 Throughput maximisation

Figure 5.6 shows a zoomed-in section (from t = 3 h to the end of the simulation) of the seven-hour simulation, focusing on the scenario where the CVs are maintained at setpoint but the HNMPC maximises THP by switching on an additional hydrocyclone.

The discussion of the increased THP as a result of the increased hydrocyclone cluster capacity is given in Section 5.4.3. However, the zoomed-in graphs clearly show how soon after the feed ore hardness reduction and *PSE* setpoint decrease the controller maximises THP. Figure 5.6 also shows that the disturbance of α_r is easily rejected, even while THP is being maximised. During this time both controllers maintain *PSE* and the monetary benefit will be a result of the increased THP and not a result of increased recovery due to a higher *PSE* as in Section 5.4.4.1. The monetary benefit from being able to switch hydrocyclones to increase THP is calculated from (5.3) as

$$\psi_{NMPC} = 7295.02 \text{ \$/h}$$

$$\psi_{HNMPC} = 7854.04 \text{ \$/h}$$

$$\text{Economic benefit} = 559.02 \text{ \$/h}.$$

This equates to a per hour monetary improvement of 8% due to the increased throughput.

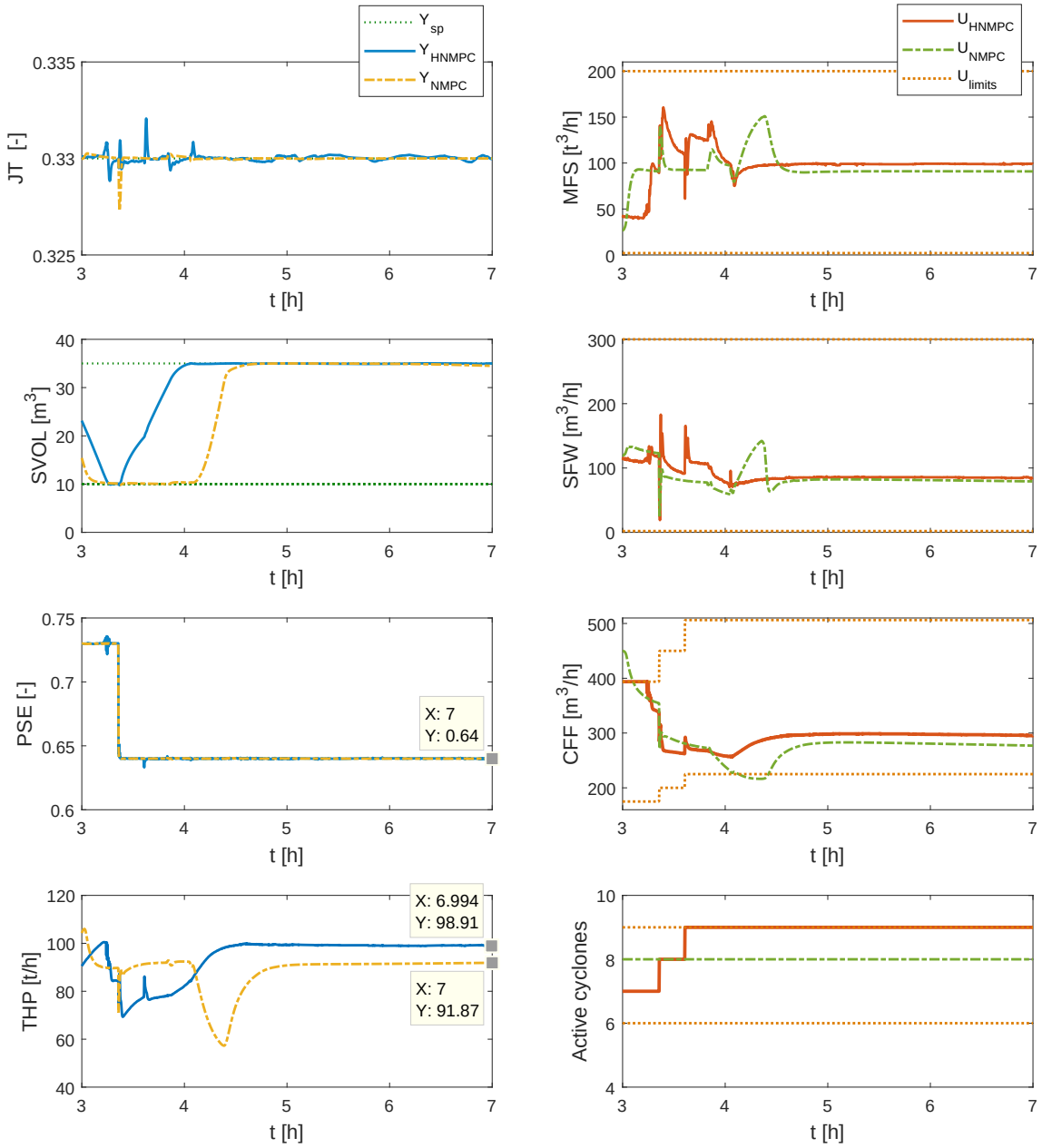

Figure 5.6. Comparison of the CV and *THP* responses for the HNMPC and NMPC with a reduced *PSE* setpoint and softer feed ore.

5.4.5 HNMPC with state noise results

This chapter has clearly illustrated the benefits of using an HNMPC that can use the hydrocyclone cluster to achieve a better steady-state or to optimise the grinding mill circuit. A final test is conducted to show that for a practical implementation, with a state estimator similar in performance to those in

[42, 50, 51, 52], which can estimate the states and parameters to within 2%, the controller will still provide similar results to the noiseless simulation.

The results of the HNMPC with THP maximisation when 2% state noise is added are shown in Figure 5.7. The figure shows that all CVs are controlled even when the controller needs to implement more high-frequency control moves to compensate for the state/measurement noise.

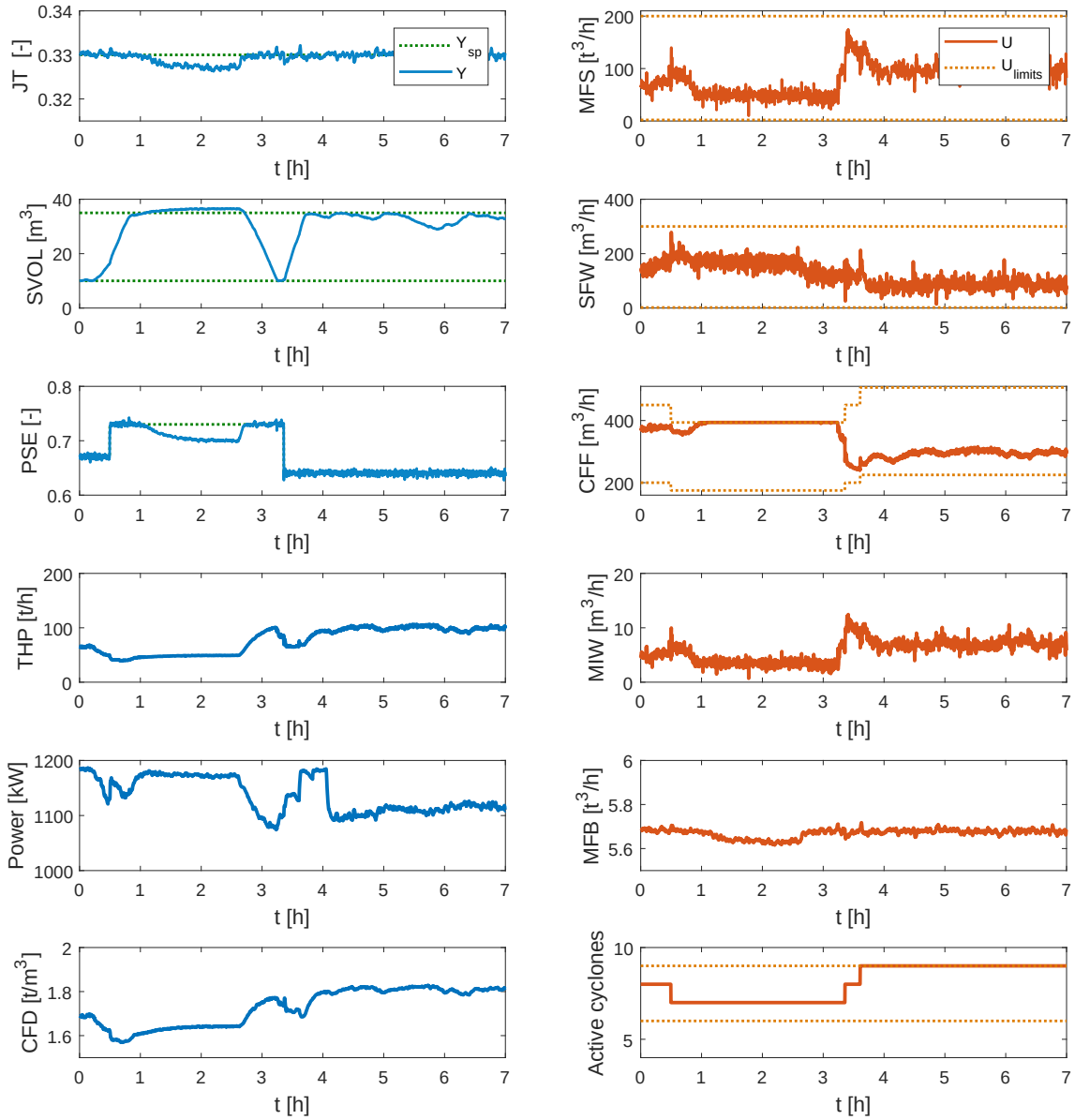

Figure 5.7. Simulation results for the HNMPC with THP maximisation when 2% normally distributed state noise is added.

A comparison of the performance metrics for the HNMPC with full-state feedback and the HNMPC with normally distributed state noise is given in Table 5.2. The results show an increase in PSE and J_T error, but this is expected with the addition of state noise. The controller takes the same control action trajectories for the low-frequency disturbances, setpoint changes and optimisation opportunities as when full-state feedback is assumed, but per iteration the outputs are controlled with high-frequency control moves to reject the continuous process noise. The results therefore indicate that for a practical implementation, the full-state feedback advantages as discussed in this chapter are still viable.

Table 5.2. Controller performance

Metric	HNMPC with full-state feedback	HNMPC with 2% state noise
$PSE_{Performance}$	0.1173	0.31
$J_{Tperformance}$	0.0025	0.0042
$THP_{Average}$	76.26 t/h	76.49 t/h

5.4.6 Controller execution time

The controller was simulated with MATLAB R2017a on personal desktop computer with an Intel Core i7-3930k 3.2GHz processor with 8 GB RAM. The HNMPC controller took on average 0.3 seconds to solve in the case where the minimum function tolerance was reached. However, in the case where the controller reached its maximum number of generations, it took at most six seconds. These controller execution times are much less than the sampling time of 10 seconds and are suitable for practical implementation. It could be argued that the controller settings can be adjusted so that the maximum number of generations is increased, since it could result in a potential better candidate solution and there are four seconds available for additional processing. This assumption was tested by increasing the population size and maximum number of generations, but it was found that the controller could not achieve the desired fitness function value because of the length of N_p and the presence of two integrating models. Therefore, even with an infinite amount of control moves, the desired minimum fitness function value cannot be obtained.

5.5 CONCLUSION

In this chapter the simulation results of four simulations were presented. The simulations were set up in a systematic way to show the advantages of NMPC. The NMPC showed that with large disturbances the plant can be controlled. The second simulation showed that the HNMPC can also benefit from being able to predict the non-linear system dynamics and could therefore also control the plant adequately. However, since it could switch hydrocyclones, in the case of hard feed ore and an optimistic *PSE* target, the HNMPC achieved a better steady-state condition.

The third simulation showed that a linear optimisation objective can be added to the objective function and that by carefully choosing the controller weights (as chosen in Chapter 4) the controller can regulate the setpoints and maximise throughput. The first three experiments all assumed full-state feedback. This ensured that the comparison of the NMPC to the HNMPC was not biased by any external factors. Therefore, any advantages shown were purely from the HNMPCs ability to switch hydrocyclones.

The third simulation was re-run but with 2% normally distributed state noise to illustrate the practical validity of the controller. The simulation with state noise showed that the controller could still maintain all the benefits it offered with full-state feedback, while controlling the high-frequency noise.

Controller execution time is known to be an issue [4], and under the worst case scenario the HNMPC with THP maximisation only takes 60% of the controller execution interval to find the best set of control actions.

CHAPTER 6 CONCLUSION

6.1 CONCLUDING REMARKS

With the design and simulation of an HNMPC controller the initial hypothesis was proven true: An HNMPC controller can be used to control a grinding mill circuit while benefiting from using discrete dynamics as an additional controller handle. The switching of hydrocyclones proved to be a good additional handle in situations where the hardness and composition of feed ore to a grinding mill circuit changes and the quality setpoint is regularly changed. Certain optimisation benefits can also be achieved with the additional MV.

From the literature available on grinding mill circuit control, it is evident that the field is continuously expanding, not merely toward newer control technologies, but also toward including previously ignored or segregated MVs. To address the gap of predictive controllers not including the switching of hydrocyclones, a grinding mill model was expanded to a hybrid model. The model parameters were refitted and a qualitative step test showed that the refitting was successful.

An HNMPC controller was designed using the full hybrid model and a GA. The controller was compared to a base case NMPC. Even though NMPC is considered one of the best control techniques for grinding mill circuits, with harder than nominal feed ore and an increase in the *PSE* setpoint the NMPC cannot reach the setpoint. This indicates that the current state-of-the-art controllers for grinding mill circuits might not be able to achieve certain setpoints (from a plantwide controller) as they are limited by control handles. The HNMPC could use the additional discrete dynamics to achieve a better operating condition than the NMPC.

In the case where the feed ore hardness was below nominal, the grinding mill circuit could operate at a

much higher capacity, but it is limited to the cluster capacity for the NMPC. The HNMPC was able to increase the capacity by switching hydrocyclones, and while all setpoints were maintained the plant throughput was significantly increased. The HNMPC could reduce the sum of errors squared of *PSE* over the seven-hour simulation by more than 70% and throughput was increased by 5.4%.

The GA proved to be a very robust algorithm for controller solution because of its stochastic nature in generating new populations. The controller could very quickly solve the control problem and never exceeded any constraints. The controller remained stable over the extreme disturbance changes in the simulation along with large *PSE* setpoint changes, even in the presence of added state noise.

6.2 FUTURE WORK

This study considered one of the possible discrete MV elements in the grinding mill circuit. However, based on the successful implementation of the HNMPC using a GA, there are various interesting topics and gaps that should be investigated. Some of these topics are the following

- In this study it was assumed that a plantwide controller will use *PSE* as a handle to stabilise downstream processes. One of the future topics could be to include a plantwide controller utilising a cascaded HNMPC configuration. A master plantwide HNMPC controller can set the targets for the slave HNMPC targets. With this configuration, not only can discrete dynamics be controlled as part of the optimal solution, but discrete events such as fixed maintenance intervals of a grinding stage can be added to the controller as disturbance variables.
- Full-state feedback was assumed in this study, and in one simulation normally distributed noise was added to the states to emulate state estimation. This study can be reproduced, but with a complete hybrid state and disturbance estimator included in the feedback loop.
- A fault-tolerant controller can firstly detect a fault on one of the control handles, then identify it. The fault-tolerant controller then evaluates over a receding horizon whether it will be economically feasible to shut down the plant or to continue running with the fault [65]. Instead of using fault-tolerant NMPC as in [65], fault-tolerant HNMPC could use the discrete dynamics to compensate for the continuous fault. For example, if CFF gets stuck to its running value, *PSE* can still be controlled by switching hydrocyclones.

- A more complete HNMPC can be formulated to include more optimisation objectives (such as minimising the mill power) and to include more discrete dynamics in order to achieve the additional controller objectives. Additional discrete dynamics that can be added to the circuit are selecting which feedstock to use for the mill, which mills are active in a parallel configuration or if a secondary grinding stage is active or not in a series configuration.

REFERENCES

[1] J. D. le Roux, I. K. Craig, D. G. Hulbert, and A. L. Hinde, "Analysis and validation of a run-of-mine ore grinding mill circuit model for process control," *Minerals Engineering*, vol. 43-44, pp. 121–134, 2013.

[2] X. Chen, J. Zhai, S. Li, and Q. Li, "Application of model predictive control in ball mill grinding circuit," *Minerals Engineering*, vol. 20, no. 11, pp. 1099–1108, 2007.

[3] D. Hodouin, "Methods for automatic control, observation, and optimization in mineral processing plants," *Journal of Process Control*, vol. 21, no. 2, pp. 211–225, 2011.

[4] L. C. Coetzee, I. K. Craig, and E. C. Kerrigan, "Robust nonlinear model predictive control of a run-of-mine ore milling circuit," *IEEE Transactions on Control Systems Technology*, vol. 18, no. 1, pp. 222–229, 2010.

[5] B. Matthews and I. K. Craig, "Demand side management of a run-of-mine ore milling circuit," *Control Engineering Practice*, vol. 21, no. 6, pp. 759–768, 2013.

[6] I. K. Craig, D. G. Hulbert, G. Metzner, and S. P. Moult, "Optimized multivariable control of an industrial run-of-mine milling circuit," *Journal of the South African Institute of Mining and Metallurgy*, vol. 92, no. 6, pp. 169–176, 1992.

[7] D. Wei and I. K. Craig, "Grinding mill circuits: A survey of control and economic concerns," *International Journal of Mineral Processing*, vol. 90, no. 1-4, pp. 56–66, 2009.

[8] B. Muller and P. L. D. Vaal, "Development of a model predictive controller for a milling circuit," *Journal of the South African Institute of Mining and Metallurgy*, vol. 100, no. 7, pp. 449–454, 2000.

[9] M. Hadizadeh, A. Farzanegan, and M. Noaparast, "Supervisory fuzzy expert controller for SAG mill grinding circuits: Sungun copper concentrator," *Mineral Processing and Extractive Metallurgy Review*, vol. 38, no. 3, pp. 168–179, 2017.

[10] M. S. Powell, A. P. van der Westhuizen, and A. N. Mainza, "Applying grindcurves to mill operation and optimisation," *Minerals Engineering*, vol. 22, no. 7-8, pp. 625–632, 2009.

[11] I. K. Craig, D. G. Hulbert, G. Metzner, and S. P. Moult, "Extended particle-size control of an industrial run-of-mine milling circuit," *Powder Technology*, vol. 73, pp. 203–210, 1992.

[12] S. Botha, I. K. Craig, and J. D. le Roux, "Switching cyclones to increase product particle size range for ore milling circuits," in *IFAC Workshop on Automation in Mining, Minerals and Metal Industry, Oulu, Finland, 25-27 Aug., 2015. IFAC-PapersOnLine*, vol. 28, issue 17, 2015, pp. 92–97.

[13] F. Estrada, "Hybrid model predictive control for grinding plants," in *19th IFAC World Congress, Cape Town, South Africa, 24-29 Aug., 2014. IFAC Proceedings Volumes*, vol. 47, issue 3, 2014, pp. 11 512–11 517.

[14] M. A. Naidoo, R. Padhi, and I. K. Craig, "A new nonlinear suboptimal control design approach for milling circuits," in *19th IFAC World Congress, Cape Town, South Africa, 24-29 Aug., 2014. IFAC Proceedings Volumes*, vol. 47, issue 3, 2014, pp. 9804–9809.

[15] J. D. le Roux, L. E. Olivier, M. A. Naidoo, R. Padhi, and I. K. Craig, "Throughput and product quality control for a grinding mill circuit using non-linear MPC," *Journal of Process Control*, vol. 42, pp. 35–50, 2016.

[16] R. P. King, *Modeling and simulation of mineral processing systems*. Boston: Elsevier Science, 2012.

[17] S. Strohmayr and W. Valery Jr, "SAG mill circuit optimisation at Ernest Henry Mining," in *Proceedings of the SAG 2001 Conference, Vancouver, BC, Canada*, vol. 30, 2001.

[18] D. Cirulis and J. Russell, "Cyclone monitoring system improves operations at KUC's Copperton concentrator," *Engineering and Mining Journal*, vol. 212, no. 10, pp. 44–49, 2011.

[19] D. Xiao, D. Song, L. Peng, and T. Li, "Hybrid model predictive control based on modified particle swarm optimization," in *Proceedings Bio-Inspired Computing: Theories and Applications (BIC-TA), IEEE Fifth International Conference, Changsha, China, 23-26 Sept.*, 2010, pp. 385–390.

[20] C. J. Muller and I. K. Craig, "Economic hybrid non-linear model predictive control of a dual circuit induced draft cooling water system," *Journal of Process Control*, vol. 53, pp. 37–45, 2017.

[21] P. Karelovic, E. Putz, and A. Cipriano, "A framework for hybrid model predictive control in mineral processing," *Control Engineering Practice*, vol. 40, pp. 1–12, 2015.

[22] T. J. Napier-Munn, S. Morrell, R. D. Morrison, and T. Kojovic, *Mineral comminution circuits: Their operation and optimisation*. Australia: Julius Kruttschnitt Mineral Research Centre, University of Queensland, 1996, vol. 2.

[23] I. K. Craig and I. M. MacLeod, "Specification framework for robust control of a run-of-mine ore milling circuit," *Control Engineering Practice*, vol. 3, no. 5, pp. 621–630, 1995.

[24] G. G. Stanley, *The extractive metallurgy of gold in South Africa*. Johannesburg: South African Institute of Mining and Metallurgy, 1987, vol. 7.

[25] D. Wei and I. K. Craig, "Economic performance assessment of two ROM ore milling circuit controllers," *Minerals Engineering*, vol. 22, no. 9-10, pp. 826–839, 2009.

[26] M. Maleki-Moghaddam, M. Yahyaei, and S. Banisi, "Converting AG to SAG mills: The Gol-E-Gohar iron ore company case," *Powder Technology*, vol. 217, pp. 100–106, 2012.

[27] J. T. Kalala, M. Breetzke, and M. H. Moys, "Study of the influence of liner wear on the load behaviour of an industrial dry tumbling mill using the discrete element method (DEM)," *International Journal of Mineral Processing*, vol. 86, no. 1-4, pp. 33–39, 2008.

[28] M. S. Powell, N. S. Weerasekara, S. Cole, R. D. LaRoche, and J. Favier, "DEM modelling of liner evolution and its influence on grinding rate in ball mills," *Minerals Engineering*, vol. 24, no. 3, pp. 341 – 351, 2011.

[29] I. K. Craig and I. M. MacLeod, "Robust controller design and implementation for a run-of-mine ore milling circuit," *Control Engineering Practice*, vol. 4, no. 1, pp. 1–12, 1996.

[30] D. Hulbert, "Evaluation of the economic benefits of milling circuit control," in *15th IFAC World Congress, Spain, Barcelona, 21-26 July, 2002. IFAC Proceedings Volumes*, vol. 35, issue 1, 2002, pp. 77–82.

[31] D. Wei, "Development of performance functions for economic performance assessment of process control systems," PhD Thesis, University of Pretoria, 2010.

[32] L. C. Coetzee, "Stabilising and optimising a primary closed-loop milling circuit feeding a flotation circuit using StarCS RNMPC," in *19th IFAC World Congress, Cape Town, South Africa, 24-29 Aug., 2014. IFAC Proceedings Volumes*, vol. 47, issue 3, 2014, pp. 9786–9791.

[33] D. Hodouin, S.-L. Jämsä-Jounela, M. Carvalho, and L. Bergh, "State of the art and challenges in mineral processing control," *Control Engineering Practice*, vol. 9, no. 9, pp. 995–1005, 2001.

[34] M. L. Darby and M. Nikolaou, "MPC: Current practice and challenges," *Control Engineering Practice*, vol. 20, no. 4, pp. 328–342, 2012.

[35] S. J. Qin and T. A. Badgwell, "A survey of industrial model predictive control technology," *Control Engineering Practice*, vol. 11, no. 7, pp. 733–764, 2003.

[36] R. E. McIvor and J. A. Finch, "A guide to interfacing of plant grinding and flotation operations," *Minerals Engineering*, vol. 4, no. 1, pp. 9–23, 1991.

[37] C. Sosa-Blanco, D. Hodouin, C. Bazin, C. Lara-Valenzuela, and J. Salazar, "Economic optimization of a flotation plant through grinding circuit tuning," *Minerals Engineering*, vol. 13, no. 10, pp. 999–1018, 2000.

[38] C. Munoz and A. Cipriano, "Integrated system for supervision and economic optimal control of mineral processing plants," *Minerals Engineering*, vol. 12, no. 6, pp. 627–643, 1999.

[39] J. D. le Roux, S. Skogestad, and I. K. Craig, "Plant-wide control of grinding mill circuits: Top-down analysis," in *17th IFAC Symposium on Control, Optimization and Automation in Mining, Mineral and Metal Processing MMM, Vienna, Austria, 31 Aug-2 Sep 2016. IFAC-PapersOnLine*, vol. 49, issue 20, 2016, pp. 72–77.

[40] S. Skogestad, "Plantwide control: The search for the self-optimizing control structure," *Journal of Process Control*, no. 5, pp. 1–30, 2000.

[41] A. V. E. Conradie and C. Aldrich, "Neurocontrol of a ball mill grinding circuit using evolutionary reinforcement learning," *Minerals Engineering*, vol. 14, no. 10, pp. 1277–1294, 2001.

[42] T. A. Apelt, S. P. Asprey, and N. F. Thornhill, "Inferential measurement of SAG mill parameters II: State estimation," *Minerals Engineering*, vol. 15, no. 12, pp. 1043–1053, 2002.

[43] S. Morrell, "A new autogenous and semi-autogenous mill model for scale-up, design and optimisation," *Minerals Engineering*, vol. 17, no. 3, pp. 437–445, 2004.

[44] J. D. le Roux and I. K. Craig, "Reducing the number of size classes in a cumulative rates model used for process control of a grinding mill circuit," *Powder Technology*, vol. 246, pp. 169–181, 2013.

[45] K. Nageswararao, D. M. Wiseman, and T. J. Napier-Munn, "Two empirical hydrocyclone models revisited," *Minerals Engineering*, vol. 17, no. 5, pp. 671–687, 2004.

[46] L. R. Plitt, "A mathematical model of the hydrocyclone classifier," *CIM Bulletin*, vol. 69, no. 776, pp. 114–123, 1976.

[47] J. D. le Roux, A. Steinboeck, A. Kugi, and I. K. Craig, "An EKF observer to estimate semi-autogenous grinding mill hold-ups," *Journal of Process Control*, vol. 51, pp. 27–41, 2017.

[48] C. Bouché, C. Brandt, A. Broussaud, and W. Drunick, "Advanced control of gold ore grinding plants in South Africa," *Minerals engineering*, vol. 18, no. 8, pp. 866–876, 2005.

[49] M. A. Naidoo, L. E. Olivier, and I. K. Craig, "Combined neural network and particle filter state estimation with application to a run-of-mine ore mill," in *10th International Symposium on Dynamics and Control of Process Systems, Mumbai, India, 18-20 Dec., 2013. IFAC Proceedings Volumes*, vol. 46, issue 32, 2013, pp. 397–402.

[50] L. E. Olivier, B. Huang, and I. K. Craig, "Dual particle filters for state and parameter estimation with application to a run-of-mine ore mill," *Journal of Process Control*, vol. 22, no. 4, pp. 710–717, 2012.

[51] L. E. Olivier, I. K. Craig, and Y. Q. Chen, "Fractional order and BICO disturbance observers for a run-of-mine ore milling circuit," *Journal of Process Control*, vol. 22, no. 1, pp. 3–10, 2012.

[52] J. A. Herbst and W. T. Pate, "Object components for comminution system softsensor design," *Powder Technology*, vol. 105, no. 1-3, pp. 424–429, 1999.

[53] A. Bemporad and M. Morari, "Control of systems integrating logic, dynamics, and constraints," *Automatica*, vol. 35, no. 3, pp. 407–427, 1999.

[54] S. Zhang and X. Xia, "Optimal control of operation efficiency of belt conveyor systems," *Applied energy*, vol. 87, no. 6, pp. 1929–1937, 2010.

[55] C. J. Muller and I. K. Craig, "Energy reduction for a dual circuit cooling water system using advanced regulatory control," *Applied Energy*, vol. 171, pp. 287–295, 2016.

[56] E. Putz and A. Cipriano, "Hybrid model predictive control for flotation plants," *Minerals Engineering*, vol. 70, pp. 26–35, 2015.

[57] W. P. M. H. Heemels, B. D. Schutter, and A. Bemporad, "Equivalence of hybrid dynamical models," *Automatica*, vol. 37, no. 7, pp. 1085–1091, 2001.

[58] D. E. Seborg, T. F. Edgar, D. A. Mellichamp, and F. J. Doyle, *Process dynamics and control*, 3rd ed. New York: John Wiley & Sons, 2010.

[59] F. D. Torrisi and A. Bemporad, "HYSDEL: A tool for generating computational hybrid models for analysis and synthesis problems," *IEEE Transactions on Control Systems Technology*, vol. 12, no. 2, pp. 235–249, 2004.

[60] D. Whitley, "A genetic algorithm tutorial," *Statistics and Computing*, vol. 4, no. 2, pp. 65–85, 1994.

[61] A. A. A. Esmin, G. Lambert-Torres, and A. C. Zambroni de Souza, "A hybrid particle swarm optimization applied to loss power minimization," *IEEE Transactions on Power Systems*, vol. 20, no. 2, pp. 859–866, 2005.

[62] K. Mitra and R. Gopinath, "Multiobjective optimization of an industrial grinding operation using elitist nondominated sorting genetic algorithm," *Chemical Engineering Science*, vol. 59, pp. 385–396, 2004.

[63] F. N. Shi and T. J. Napier-Munn, "Effects of slurry rheology on industrial grinding performance," *International Journal of Mineral Processing*, vol. 65, no. 3, pp. 125–140, 2002.

[64] C. E. Garcia, D. M. Prett, and M. Morari, "Model predictive control: Theory and practice: A survey," *Automatica*, vol. 25, no. 3, pp. 335–348, 1989.

[65] L. E. Olivier and I. K. Craig, "Should I shut down my processing plant? An analysis in the presence of faults," *Journal of Process Control*, vol. 56, pp. 35–47, 2017.